INTERSTITIAL CHANGES AND THEIR RESOLUTION AFTER ULTRASOUND GUIDED RADIOFREQUENCY INDUCED ABLATION IN PORCINE LIVER

BY

ANDRZEJ K. BUCZKOWSKI

MD, Pomeranian Medical School, Szczecin, Poland, 1983

A THESIS SUBMITTED IN PARTIAL FULFILMENT OF THE REQUIREMENTS FOR THE DEGREE OF

MASTER OF SCIENCE IN SURGERY

THE FACULTY OF GRADUATE STUDIES

(Department of Surgery, University of British Columbia)

THE UNIVERSITY OF BRITISH COLUMBIA

APRIL 2003

INTERSTITIAL CHANGES AND THEIR RESOLUTION AFTER ULTRASOUND GUIDED RADIOFREQUENCY INDUCED ABLATION IN PORCINE LIVER

BY

ANDRZEJ K. BUCZKOWSKI

MD, Pomeranian Medical School, Szczecin, Poland, 1983

A THESIS SUBMITTED IN PARTIALFULFILMENT OF THE REQUIREMENTS FOR THE DEGREE OF

MASTER'S OF SURGERY

In

THE FACULTY OF GRADUATE STUDIES

(Department of Surgery, University of British Columbia)

THE UNIVERSITY OF BRITISH COLUMBIA

APRIL 2003

In presenting this thesis in partial fulfilment of the requirements for an advanced degree at the University of British Columbia, I agree that the Library shall make it freely available for reference and study. I further agree that permission for extensive copying of this thesis for scholarly purposes may be granted by the head of my department or by his or her representatives. It is understood that copying or publication of this thesis for financial gain shall not be allowed without my written permission.

Department of Surgery

The University of British Columbia
Vancouver, Canada

Date April 16/03

DE-6 (2/88)

ABSTRACT

Background:

Radiofrequency ablation (RFA) is a new minimally invasive technique for the treatment of primary and secondary liver tumours. No complications have been reported to date in cases of experimental application involving animal (guinea pig, rat, porcine) models, however previous studies have not specifically addressed its safety in relation to changes induced in the normal hepatic parenchyma surrounding the lesion treated by RFA.

Methods:

Radiofrequency ablation was performed in both the right and left liver lobes of 28 female domestic swine. The animals were divided into four groups based on the attempted thermal injury to: hepatic veins; portal veins and bile ducts; diaphragm; and injury resulting from excessive radiofrequency (RF) energy delivery. RF lesions were followed with ultrasound examination, and gross and histologic examination was performed on the left lobe lesions on day 3 and the right lobe lesions on day 30.

Results:

There was no evidence of injury to main hepatic or portal vessels or bile ducts. Superficial and deep diaphragmatic burns were observed on day 3, but these were all completely healed by day 30. Full-thickness burns of the stomach and jejunum (one case of each) were encountered in separate experiments. There were no treatment-related deaths. No bile leak, bilomas, bleeding or abscesses were observed. The histologic pattern of RFA induced necrosis and tissue healing was consistent through all the cases and was related to the amount of energy delivered to the experiment area. Ultrasound proved to be an efficient method in RF probe placement and initial treatment, however its follow-up accuracy declines with the time after the RFA.

Conclusions:

Hepatic RFA is a safe procedure. No serious complications were observed with intrahepatic ablations. Thermal injuries were however produced in contiguous extrahepatic structures, when RFA was applied to superficial, subcapsular liver. These observations suggest the need for extreme attention during the treatment sessions and evaluation of laparoscopy as the preferred mode of the RF ablation delivery.

TABLE OF CONTENTS

LIST OF FIGURES

Tables:

CHAPTER ONE

1. INTRODUCTION

1.1 INRODUCTION TO LIVER CANCER

1.1.1 Liver cancer

The malignancies of liver tissue are common with a worldwide incidence. Hepatocellular carcinoma (HCC) is one of the most common solid cancers. It is the fifth most common fatal cancer in men and the eighth in women [1,2]. The non-Western population incidence of HCC is related to predominance of hepatitis B infection and in lesser degree to dietary aflatoxins. Western societies typically experience the liver cancer in the form of metastases mostly due to progressing colorectal cancer. There is a much smaller percentage incidence of alcohol and chronic hepatitis C induced HCC. Hepatic metastases occur in 40 – 50% of adult patients with extrahepatic primary malignancy. The most common metastases originate within portal vein system mostly from colorectal cancer. Extraabdominal sources include breast cancer, lung cancer and metastatic cutaneous melanomas.

1.1.2 Survival and recurrence

The overall survival rate of primary HCC is low. Development of newer modalities of treatment brings a hope for liver cancer patients to achieve at least a prolonged survival. Less than 30% of patients are candidates for curative surgical resection at the time of presentation [3,4]. In metastatic malignancies the patients' prognosis are determined by the volume of liver tissue replaced by the cancer. The greater the volume replaced by tumour the worse is the survival outlook. At the present time in North America about 50% of patients survive 3 months after the onset of the symptoms. Less than 10% of patients survive 1 year or longer [5]. The cases of long-term survival have been achieved through the resection of liver metastases. The improved results are in direct relationship to earlier diagnosis and patient selection. Tests such as spiral CT, T1 and T2-weight MRI are useful to evaluate neoplasms of all types. Appropriate clinical follow-up at regular intervals coordinated with serum levels of CEA tumour marker may detect early recurrence of colorectal cancer. As a result multiple, sequential/interval resections have resulted in survivals of up to 20 years [5,6,7]. On the other hand the scrupulous follow up including AFT (alfa-feto protein) serum measurements and liver US in patients with Hepatitis B and C chronic infection have resulted in the diagnosis and successful treatment of hepatocellular carcinoma in its earlier stages. In cases of liver metastases due to functioning endocrine tumours the liver resection is a very efficient therapeutic method to control symptoms of functioning tumour, as they are generally slow-growing lesions. Among many patients, however there is a group of poor candidates for surgical therapy mostly due to either co-morbid illnesses, advanced stage of the cancer, low functional reserve of the liver, or tumour location within the liver. Various local treatment methods for non-surgical patients have been under scientific and clinical evaluation for the last 20 years.

1.1.3 Adjuvant and interstitial treatment

Liver tumours of all the types respond poorly to chemotherapy and radiation. Beside curative resection the available therapeutic modalities include cryoablation, ultrasound, microwave and radiofrequency ablation. The simplest method of interstitial treatment utilizes the injection of 95% ethyl alcohol (ETOH) into the lesion. The basis of the clinical effectiveness is ETOH sclerosing and tissue denaturating capabilities, which leads to the tumour detraction. Its efficacy is better in the encapsulated, softer lesions of HCC than in metastatic tumours. ETOH limitations include the small size of treatable tumour (<3 cm) and side effects of alcohol due to uncontrolled diffusion of ethanol into the adjacent normal liver. An injection volume of 1 – 8 cc per treatment is commonly used [8,9]. The larger injections using more than 10 cc of alcohol, especially close to the large veins, risk the direct central vascular injection of the alcohol likely to result in transient general alcohol toxicity and localized irritation and sclerosing changes of the vein wall as well as bile ducts. Overall the main disadvantage of the ETOH injection is poor control of its volume distribution.

Cryoablation technology is a well-studied method of treatment. This method of sub-zero temperature delivery to the treatment area is non-tissue selective. It means that both the tumour and the normal liver tissue undergo the same destruction regulated by the size of the probe and number of freeze-thaw cycles [10,11,12]. Limiting factors include: significant side effects in form of bleeding, liver abscesses, biliary fistula as well as the need for bulky, expensive equipment. Despite the introduction of smaller probes and laparoscopic equipment the popularity of cryotherapy has been recently declining [13,14,15,16,17,18,19,20]. Microwave as well as interstitial ultrasound and laser therapies are still in the phase of clinical experimental evaluation [21,22]. Radiofrequency ablation has been improving and is becoming an accepted method of localized liver tumour treatment.

1.2 TREATMENT OF LIVER CANCER

1.2.1 Surgery

The surgical resection of the primary or secondary liver tumours has been considered the gold standard of treatment for any liver tumour classified as resectable. Resectability of the tumour is evaluated according to its lesion size, number of lesions, anatomic localization and co-morbid medical conditions of the patient. One of the critical aspects of the successful outcome in liver surgery is functional reserve of the liver. Patients, who are considered to be candidates for liver surgery are evaluated in order to define the functioning status of the liver by assessing the so-called liver function tests. Those include hepatocyte specific enzymes, coagulation factors, serum albumin level as well as clinical signs of ascites and hepatic encephalopathy. The patient's preoperative status is described in terms of the Pugh-Child's score and represents a perioperative mortality risk. As the underlying stage of the liver cirrhosis is a benchmark of good liver function, it is a main limiting factor precluding significant volume liver resection.

The overall resectability in HCC patients is in the range 9 – 27% [23,24]. Resectability in patients with colorectal liver metastases is 25 – 30%. Overall the long term survival in selected groups of patients after liver resection for primary liver tumours is reported at 46 – 90%, 22 – 75%, 14 – 64% at 1, 3, and 5 years after the surgery respectively [25,26,27,28]. Survival after metastatic liver cancer treated with an intent for cure resection has been reported at 83 – 93%, 50 – 60%, 28 – 50% at 1, 3, 5 years respectively [29,30,31]. Despite improving outcomes after liver resection for cure, many patients will experience recurrence of tumour within the liver remnant [30]. This subgroup then may be still evaluated for repeat resection. With each following recurrence, smaller and smaller subpopulations of patients qualify for re-resection. In the past, for most primary recurrence and re-recurrence patients the only available treatment option was palliation.

1.2.2 Adjuvant therapies

The liver tumours are not sensitive to chemotherapy and the overall response rate is in the range of 5 – 10% even with the newest adjuvant regimes [32,33]. The response rate to radiotherapy is reported to be in the range of 5%. Both of these modalities have only been applied in a limited number of cases. Local chemotherapy in the form of chemoembolization through the hepatic artery has been employed in both advanced and complicated cases of HCC. Advanced metastatic tumours may be treated in very selected cases by open or laparoscopic canulation of hepatic artery and continuous chemoperfusion of the selected liver lobe.

1.2.3 Local treatment

The large population of the patients with liver tumours, who were not candidates for curative surgery, and who previously were considered to be untreatable, stimulated development of many methods of local palliative therapy. The types of ablative therapy most often used include: ETOH and cryoablation, as well as many newer technologies still in the experimental phase like acetic acid injection [34], yttrium-90 microspheres [35], hyperthermic saline and distilled water [36], locally chemotherapeutic agents such as cisplatin/epinephrine gel [37], microwave coagulation [38], interstitial photocoagulation [21,22] and radiofrequency ablation [39,40,41,42,43,44,45,46,47,48,49,50,51]. These treatments can be given as percutaneous injections into the tumour or local application of the thermal energy.

The mode of delivery of the local treatment has been extended by increasing experience with the laparoscopic and open routes. The application of these technologies is guided by spiral CT or US in most of the cases, independently of the delivery mode (percutaneous, laparoscopic or open access).

1.2.4 Local treatment outcomes

Overall results of interstitial treatment methods have changed the approach to long-term survival of the patient with unresectable primary or secondary liver malignancy. Reported survivals for cryoablation are in the range of 33 – 77%, 12 – 32%, and 4 – 51%, at 1, 3, and 5 years after treatment respectively [52,53,54]. Chemoembolization rates are 24 – 95%, 13 – 50%, and 6 – 18% at 1, 3, and at 5 years respectively [26,55,56]. The ETOH efficacy for HCC treatment has been reported at 83 – 95%, 33 – 78%, 13 – 55% survivals at 1, 3, 5 years after the treatment respectively [55,57,58]. The wide ranges of survival quoted in the literature are primarily due to differences in inclusion criteria in each of the studies. Better outcomes are reported for smaller tumours rather than for larger ones.

1.3 LIVER

1.3.1 Anatomy

Liver anatomy has been a focus of interest for centuries. From Johannis Walaeus to Francis Glisson, Hogarth Pringle, John Cantlie and 20th century surgeons and anatomists, extensive anatomical and surgical research brought the currently recognized understanding of liver anatomy. Liver anatomy is based on its blood supply and blood drainage anatomy and their variations. Since Claude Couinaud [59,60], the concept of segmental organization of liver, segments 1 – 8, has facilitated the progress and development of liver surgery and liver transplantation. The human liver consists of two lobes, left and right. The segmental allocation follows the branches of portal vein anatomy. Left lobe of the liver consists of segments 2 and 3 medial to the left hepatic vein, and segments 4a and 4b between the origins of left hepatic and middle hepatic veins. The right lobe consists of segments 5 – 8 lateral to the middle hepatic vein. Segment 1, so called caudate lobe has its separate portal vein branches and short hepatic veins for the independent blood drainage. Each of the hepatic segments has its own main branch of the portal vein, which enters the segment centrally. Overall the human liver mass does not present itself as fragmented structure, and to the contrary it appears to be of uniform shape. Lack of external segmentation makes it a better tissue environment facilitating interstitial treatment techniques of liver tumours.

1.3.2 Histology and pathophysiology

The liver is a wedge-shaped organ covered by a uniform thin fibrous capsule. Its weight approximates 1.5 kilograms in the adult. Dual blood supply is provided through branches of the celiac axis in the form of left and right hepatic arteries, which deliver oxigenated blood, while venous blood is delivered trough portal vein branches originating in the much of the alimentary tract, including stomach, small and large bowel with rectum and the spleen. The liver cells (hepatocytes) are the main part of the liver anatomy occupying most of its volume. The cells are arranged as one cell thick plates, bordering the vascular sinusoids through which the mixed arterial and portal blood flows. The cells are separated from the sinusoids by a thin fenestrated (porous) barrier of cells (endothelial cells and phagocytes Kupffer cells) and the space of Disse. Liver cells abutting the space of Disse do not have a continuous membrane facilitating the free interchange of molecules at the liver cell membrane. Blood, after completing its passage through the vascular sinusoids, drains into hepatic vein branches (central veins or terminal hepatic venules). Bile formed by the liver cells is secreted from the cells into minute canaliculi. They run along the centre of the liver cell plates to drain into the bile duct branches within the portal tracts. The portal tracts contain branches of: the bile duct, the hepatic artery, and the portal vein. At the confluence of main branches these constitute the portal triad. The triad all along its course is supported by collagen-rich connective tissue. The microanatomy of the liver can be regarded as consisting of either acini or lobules. The acini are centred on the axial vessels, emanating from the hepatic artery and portal venous channels in the adjacent portal tract. The acinar periphery is demarcated by the surrounding hepatic veins. Lobules are centred on terminal hepatic venules (central veins) and their peripheries are demarcated by imaginary lines joining each of the surrounding portal tracts. The portal tracts are circumscribed by a boundary of liver cells, known as the 'limiting plate'. This boundary is breached in certain forms of chronic liver disease or liver injury and thus its injury foreshadows progression to cirrhosis. The liver cells have ultrastructural characteristics of cells involved in a variety of metabolic functions. Regeneration in damaged liver occurs because of proliferation of reserve cells (oval cells) located within the liver plates. Mature hepatocytes are stable and they are not normally replicating. However, when induced by injury the regenerative capacity of oval cells is vital in the recovery of the patient with liver disease. When the damage is persistent or occurs repeatedly, it can result in the loss of the normal acinar or lobular structure and its replacement by functionally inefficient regenerative nodules [61].

1.3.3 Regeneration and postsurgical recovery

Any injury to tissue will trigger an initiation of the healing process. The tissue injury healing follows certain principles regardless of where the injury occurred or what type of injury was induced. The three main phases of healing are described as inflammation, proliferation and remodelling. Each one involves certain forms of vascular and cellular response, which facilitates major events. The major events are described as a clot formation and hemostasis, growth factor elaboration, collagen deposition, and then collagen cross-linking. The phases are precisely described, and chronologic, however they overlap during the real time event of healing. The inflammatory phase starts immediately after the injury and lasts up to 7 days. It initiates a transient vascular constriction to enable hemostasis and clot formation. This is then replaced by a vasodilation phase to facilitate the cellular response. The cellular response brings neutrophils, macrophages and lymphocyte into the area of injury. Well into the inflammatory phase fibroblasts are increasingly present in the healing tissue and aid the transition to the proliferation phase. At 3 – 4 weeks after the injury the tissue enters the remodelling phase, which may last up to year according to the type of tissue and the organ of injury [62]. Practically, on day 3 after the injury one will find all cellular elements of the inflammatory phase at the highest concentration, while on day 30 the tissue changes represent the features most likely to be continued for the rest of the remodelling phase.

1.4 RADIOFREQUENCY ABLATION

1.4.1 Definition

The goal of achieving focal tissue hyperthermia has drawn attention to the application of different forms of electrical current. Radiofrequency ablation technology utilizes high frequency alternating current with frequency of oscillation between 10 kHz to 900 MHz, while by comparison the standard AM radio broadcast operates between 550 kHz and 1600 kHz [63]. Selection of the frequency has been under investigation to identify the range effective enough to create interstitial changes without collateral charring or tissue coagulation. [63,64]

1.4.2 History

The historical use of thermal energy to treat medical conditions has its roots as early as the description in the Edwin Smith papyrus (3000 B.C.) when it was applied to tumours and ulcers of the breast. Around 460 – 370 B.C. as reported by Hippocrates, it was used for the treatment of a growth on the back of the neck of one of his patients. Initial discovery of the high frequency tissue effects by d'Arsonval (1891), who described local elevation of temperature in the living tissue during the alternating current application without any pain or muscular contractions, led to development of medical diathermy and electrosurgery. The heat induction by diathermy is attributed to the resistance of the tissue rather than to increase of the temperature of the electrode itself. [65,66,67]. Studies by Riviere 1900 [68], and Beer [69,70] described in more detail the initial technical aspects of RF system specification leading to creation of the first commercial electrosurgical prototype in 1927 by Cushing and Bovie [71]. The use of the thermocouple in 1937 by Huntoon [72] to measure the tissue temperature permitted a description of the ablation field and sharp temperature drop at the periphery of the ablated tissue. Further development was stagnant until early 1970s, mostly due to a lack of technical advances, when renewed interest stimulated multiple areas of RF application.

1.4.3 Physics

The initial use of RF technology was focused on the creation of well-controlled lesions around the tip of the electrode. This was applied to treatment of brain tissue lesions and in cardiology for the interruption of the conduction system in cases of arrhythmias. In contrast to electrocautery, which is the application of a heated probe tip to the tissue, RF does not deliver heat through a heated tip of the probe. The high frequency alternating current, usually in the range of several hundreds Hz (cps), flows from the uninsulated tip of the electrode directly into the tissue. The alternation in the current polarity induces ionic agitation in the tissue, both in the intracellular fluid ions or interstitial fluid ions, which results in frictional heating of the local tissue. In essence, the tissue around the electrode, rather than the electrode itself, becomes the primary source of heat.

Heat production is defined as the difference between heat generated by RF current flow through the tissue and heat loss from the region of treatment. The exact balance between the factors for effectiveness of RF ablation, after one has assumed certain physical and electrical tissue homogeneity, is generally influenced by three elements: RF current intensity, duration of the RF application (delivery), and the distance from the tip of the electrode. The description below applies to a single tip electrode. The most limiting factor in the creation of an ablation area is the distance from the electrode. Tissue heating decreases rapidly with increasing distance from the electrode according to equation: $\mathbf{1/r^4}$, where r = radius, distance from the electrode in the form of spheroid aligned along the electrode exposed tip.

The intensity (**I**) of the RF current influences the heat generation as $\mathbf{I^2}$, however there has to be a time period allowed for a diffusion of the delivered heat to the outer limits of the attempted lesion. Any extreme variation either too low or excessively high intensity will result in a suboptimal volume of created lesion. If the current intensity is too low, than by the definition the ablated lesion will be small. When the current intensity is too high or applied too rapidly the one of two effects will be experienced: the heating will be so intense that solidification and char formation will quickly limit further current flow due to increased tissue impedance and as a result the heat delivery to the periphery of the lesion will be compromised; too rapid spread of heat through the lesion will produce scattered areas of explosive water vaporization, resulting in unpredictable mechanical damage to tissue, and creating irregular-shaped lesions with the possibility of larger volume of destroyed tissue than desired.

Time (**T**) of application influences directly the outcome of the RF ablation. Its effect is significant in the phase of initial energy delivery and later during the phase of sustainable heat until the time required for the tissue proteins denaturation is reached.
The amount of the heat generation may be described in most simplified equation as regulated by the:

$$1/r^4 x I^2 x T$$

While heat is generated in the tissue, it is also continuously lost. The basic means of heat loss include conduction (diffusion), convection (via the circulation) and low resistance shunting (intravascular fluids, collateral tissue interfaces like liver capsule, diaphragm, renal capsule etc.).
The effect of the electrode size is considerable but it has technical limitations. The lesion volume around the straight electrode can be calculated using the formula for hemiellipse:

$$Volume = (1/2) \times (4/3) \times Pi \times (L/2) \times (D/2) \times (W/2) = 0.262 \times L \times W \times D$$

Where: L = length, W =width, D = depth

This equation becomes much more complex in cases of multi-prong and large electrodes, where the many additional components start influencing the effectiveness of RF technology.

As the single electrode RF lesions are limited by the physics of the electrode, RF current and tissue electrical characteristics, larger lesions like tumours in the liver, kidney, or bones are not preferred candidates for initial application of RF technology. With the progress in the electrode technology in the form of the multiple probes and then the multi-prong probe, improved RF devices were developed and evaluated for their experimental and clinical efficacy. The multi-electrode model, especially with curved, memory-shaped construction adds some new dimension to the physics of RF ablation compared to the single electrode models. The effectiveness of RF ablation depends on the distribution of the isotherms across the lesion. For the purpose of theoretical calculation the absorption rate density (ARD) is calculated to identify the absorbed power per unit of volume of tissue. The ARD is extremely significant in the organs with high blood flow because the patterns of vascular anatomy and vessel size are critical in heat loss during the ablation. The experimental and theoretical models were developed in the 1980s [65]. The higher the tissue blood flow a smaller distance between the electrodes has to be selected. The wider spread electrodes may create areas of coagulative necrosis around the electrode shaft with non-ablated areas between. This phenomenon was to be observed during this study of liver tissue.

Blood flows in cancer tissue vary according to the size and the type of the cancer. The rates of blood flow through a HCC mass are much higher than ones through metastases of colorectal cancer. The recorded rates have been measured in the range of 20 – 90 cc/100mg/min [73]. The theoretical modeling of the tumours often indicated low flow masses or shell models with no-flow central necrotic zone and high flow periphery.

1.4.4 Development of the treatment devices

The initial electrodes used in the experimental application of the RF were basically uninsulated electric probes or highly conductive metal plates. These designs allowed for an evaluation of the current characteristics and tissue response to RF ablation. The clinical application was limited to small volume ablations required for brain neoplasms and for cardiac conduction system treatment. The ablation of larger volumes of tissue was initially performed by multiple application of a single electrode or by using multiple single-electrodes simultaneously. These methods however successful, were time consuming or required complex technical support [74]. The improved technology of electric materials, especially the introduction of shape-memory materials permitted miniaturisation of the electrodes and prongs, which were then used to create multiple electrode array probes. The precise curved prongs lead to creation of probes in two major subtypes: the umbrella shape prong array and the tree shape prong array (RITA, Medical Instruments). The increasing number of the active electrodes in the probe is responsible for the successful ablation of larger tissue volumes at one treatment session. The creation of the coagulative necrosis begins around the individual prong and increases gradually in size according to the rules of current ARD (absorption rate density) until the individual areas of necrosis coalesce. With progressing time of the ablation enough energy is delivered to create the volume of necrosis occupying the tissue around and between the prongs up to its maximal volumetric size [75] (Fig. 1 and Fig. 2).

1.4.5 Clinical application

The gradual introduction of new ideas in the field of interstitial tissue ablation, especially RF technology, stimulated increased interest in using it in clinical cases. Studies of RF technology applied mostly to its electric evaluation as the single electrode model. Until the time of the present study there have been no reports available regarding tissue response to multi-prong RF electrode in a large animal model with animal survival.

1.4.6 Tissue effect of RF application

The original application of the RF electrical current was delivered through surface applied electrodes. The first volumetric necrosis of liver tissue was successfully created by Lounsberry in 1961, while using the rabbit liver as an experimental model [76]. The influence of small vessels on the size of ablation was noticed. The type of induced necrosis was described as coagulative necrosis with sharp line of demarcation. Similar observations were reported during experiments on guinea pigs' and bovine cadaveric livers [77,78]. The necrosis was described as aseptic necrosis. The long-term survival as well as the resolution of the RF induced necrosis was not evaluated in those studies.

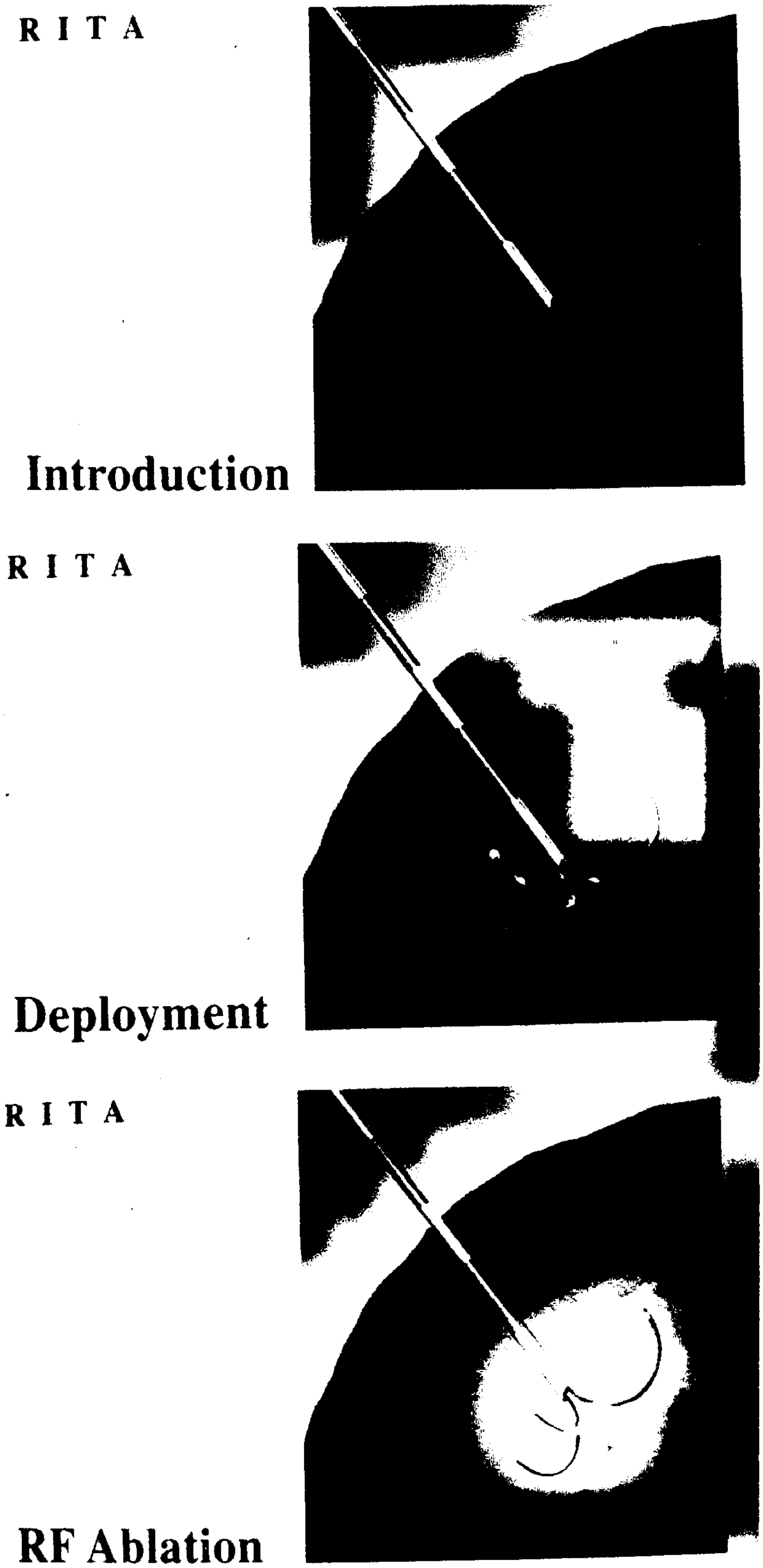

a) Placement of the probe into the liver tissue

b) Deployment of the prongs within the parenchyma

c) Volume liver tissue RF ablation

Figure 1.

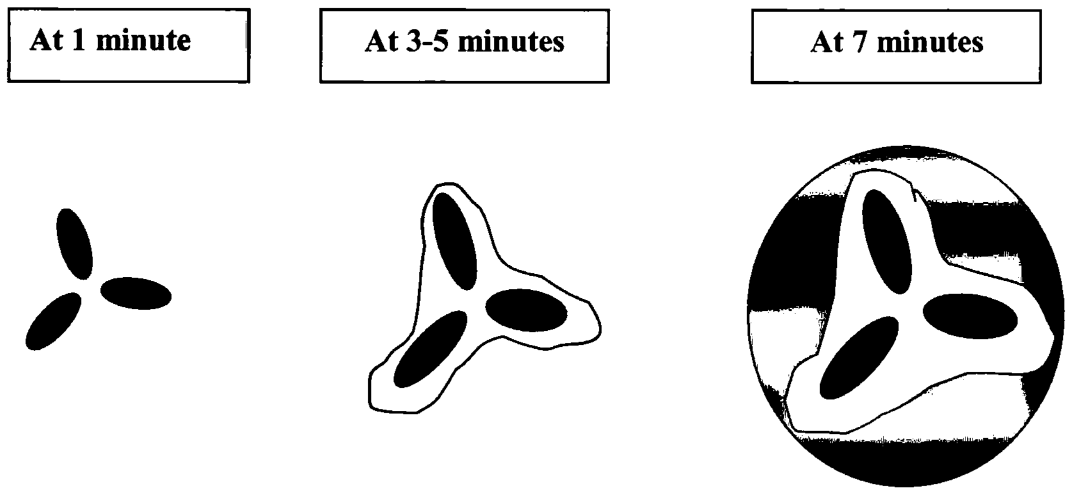

Figure 2. The illustration of the timetable of tissue changes during radiofrequency ablation. The initial coagulation necrosis is established around the prongs and with the time the diameter of the necrosis extends to eventually create the almost spherical shape of the RF ablation at 7 minutes.

1.4.7 Coagulative necrosis and radiofrequency current

The main effect of radiofrequency current flow in the tissue is heat production. It is known that a sustained temperature above 42.5°C results in tissue protein denaturisation and cell death. Translation of larger current power to larger volume of the tissue requires much more sophisticated technology and at least has to be able to sustain temperatures in range of 70 – 85°C within the treatment area to be used as a successful and reliable instrument of local ablation. Precisely calculated amounts of high power RF will deliver enough electric energy to create sufficient heat for tissue volume necrosis.

The term necrosis describes death of tissue and is irrelevant to the injury cause. Currently recognized types of the necrosis include coagulative, colliquative, caseous, gangrene, fibrinoid, and fat necrosis. A combination of the type of the tissue and nature of causative agent will determine the type of the necrosis encountered. Coagulative necrosis is observed in most of solid organs, although brain necrosis is commonly colliquative.

Coagulative necrosis is the most common form of tissue necrosis. After devitalisation, the cells retain their outline although the intracellular proteins coagulate and metabolic activity ceases. The gross appearance seen depends at least in part on the cause of the cell death, but also in part on vascular alteration particularly whether vasospam or vasodilation is encountered. Initially the texture of the tissue may be normal or firm, but later it may become soft due to autolysis. Microscopic changes are variable dependent on the time elapsed since the injury. In the first few hours after ablation normal staining with H+E is preserved, however the histochemical NADH staining will indicate arrest of mitochondrial enzymatic activity consistent with the initial stages of cellular death. Subsequent progression of necrosis will be characterized by decreasing H+E stainability of the tissue, nuclear degenerative changes and ultimately partial destruction of the cell morphology. As collagenous stroma is much more resistant to dissolution, the tissue may retain an outline of its normal structure until removal by phagocytosis. The local inflammatory response is transient and its intensity depends on the cause of necrosis. Radiofrequency created necrosis is influenced by characteristics of the delivered energy. The significant elements include the heat generation, water vapor, dissecation phenomenon, and relatively short time of volume necrosis creation [76]. The heat is created in the tissue, with tissue becoming a primary source of heat. The effective temperature, which results in protein coagulation, is reached quickly and is generally evenly spread throughout the ablated tissue volume. The interstitial fluid and its main component water reach subboiling or boiling temperature and are driven out of the tissue in the form of vapor or steam. The heat insult is completed in several minutes efficiently cutting off the blood supply to the area of treatment, especially in absence of large caliber vessels. The evolution of histologic changes within the volume of liver tissue after RF ablation at the time of inflammatory and remodelling phases of healing are at this particular moment unreported.

1.4.8 Rational of RF ablation studies on animal model

The application of a new technology is always based on the evaluation of its physical, pathophysiological and clinical outcome effects. The clinical efficacy also involves addressing the possible side effects and understanding the changes induced in the adjacent tissue. In the case of radiofrequency ablation the basic characteristics of the technology have been investigated for many years. With advancement of the technology of current conducting materials, the range of clinical applications of RFA has been expanding actively. The increase in the size of the electrodes and effective increase in the volume of tissue ablation in a short time frame introduces new elements to the understanding of tissue responses and tissue recovery after the ablation. Beside the effective treatment mode, like RFA, one has to understand and be able to avoid any complications or at least be able to identify them and prevent or reduce the existing risks.

Any possible tissue complications due to applications of RF energy will be considered to be at least a relative contraindication in clinical trials and if identified during this study will be accordingly evaluated.

It may be assumed that by the nature of technology utilized RFA is capable of inducing well-controlled lesions in an animal model. Porcine liver with its high blood flow and low fibrous tissue content resembles the anatomy and physical aspects of human liver. The specifics of RF current and its rapid drop off in peripheral temperature penetration should result in minimal pathology outside the periphery of the ablation. The vessel rich liver parenchyma may be a challenging tissue environment, especially for multi-prong electrodes. With these probe models the likelihood of interposition of large vessels or bile ducts within the RF ablation zone is high and may influence the results of treatment. The thermal injury induced by RF ablation may directly damage the anatomy and function of bile ducts, veins and arteries in the liver parenchyma. The extrahepatic organs are also considered to be at risk of injury. This includes the kidneys, adrenals, parts of gastrointenstinal (GI) tract like stomach, small bowel and transdiaphragmatic organs, particularly lung. The possible injuries to the GI tract will require separate evaluation and are outside the scope of this study.

The different study groups were selected in a specific way to simulate in the most reliable and accurate way the possible clinical scenarios, most likely expected during RF ablation in a patient. The end results will address the clinical outcome in the animals, as well as acute and chronic changes in the process of tissue response and healing after RF ablation. The histologic and gross appearance of the tissue will answer the questions of post RF ablation changes in the parenchymal tissue collateral to the ablation zone and in the ablation area in the living model.

The choice of planned evaluation on day 3 and 30 post ablation is based on the tissue response and healing in any given post surgery wound healing scenario. Day 3 represents the peak of activity in the most immediate phase after the injury. The maximum acute inflammatory response with large population of neutrophils, monocytes, fibroblasts and tissue edema is present at this time in most types of tissue. Day 30 is a point the phase of tissue recovery, which represents completed acute changes and early chronic changes. Chronic changes are well established at that time and provide indications as to future course of tissue remodelling in the future. This time frame will capture the frequency of complications such as: bleeding, organ rupture, bile leak, capsule damage, acute intravascular clot formation or the local vessel wall response occurring at day 3. The incidence of hematoma resolution, infection, abscess formation, biloma, or bile duct stricture will most effectively be evaluated at day 30. The end points of this study include survival of the animals during the first 30 days of recovery, capture of the incidence of any treatment related complications in the form of hematomas, bilomas, abscesses, and extent of the necrosis of the treated liver parenchyma and its surroundings.

1.4.9 Summary of introduction

Both primary and secondary liver cancer is a major clinical challenge. Many patients are poor candidates for surgical treatment at the time of diagnosis. The local treatment methods are being investigated for clinical use. Some like ethanol alcohol or cyroablation are used in daily practice. Their application is limited by constrains of the particular technique and its side effects. There is an on going need to develop and use new technologies in order to improve the clinical outcomes in patients with liver tumours. Among many methods radiofrequency current ablation is very promising. It has been used in the treatment of cardiac conducting system pathologies with consistent success. As the physics and tissue effects of single probe RF ablation are known from previous studies, we hypothesise that multi-prong RF probe will be successful in the creation of volume necrosis in the animal liver. Its safety and understanding of RF tissue induced changes and their recovery in liver tissue should be based on the evaluation of this technology in porcine liver model.

1.5 THESIS OBJECTIVES

The objective of this study is an evaluation of interstitial changes after RF ablation and possible injury to the intrahepatic and extrahepatic structures and organs in response to RF ablation in animal liver.

The following specific objectives consist of the:

1. Assessment of incidence of intrahepatic RFA induced changes and complications in form of:
    a. Bile leak, bilomas.
    b. Infection, abscess formation, cyst formation in the treated area.
    c. Vessel response to the ablation: thrombus, obliteration, hematoma.
    d. Diaphragmatic response to the ablation, penetration into the pleural cavity, subphrenic abscess, necrosis of the diaphragm.
2. Assessment of characteristics of RF ablation for each study group in regards of mean temperature, impedance, energy output and time required to consistently create the ablation.
3. Assessment of ultrasound imaging as RF application guiding mode and tissue evaluation tool during and post treatment follow up.
4. Assessment of histopathology tissue of RF induced ablation and patterns of injured liver tissue recovery.

Our hypothesis regarding previously specified goals are:

1. The multiple-prong RF ablation is a simple and effective mean of creating a well-demarcated volume necrosis in the normally perfused liver tissue.
2. Anatomy dependent, the electrical requirements of the RF ablation are characteristic to the area of the liver ablation and consistent with tissue pattern.
3. Despite relatively large volumes of ablation, tissue recovery is full and risks of complications within the liver parenchyma are low.
4. Ultrasound is a useful technology of the real-time guidance during the RF ablation.
5. Long-term ultrasound follow up efficacy may be somewhat limited by its own specific technology and regenerative tissue changes.

CHAPTER TWO

2.1 Animal model

2.1.1 Anatomy of the target organ

The choice of porcine liver as the study target organ is based on the size and volume of accessible liver tissue. Previous experiments were conducted on the livers of rabbits, guinea pigs [77] and rats [78]. The current stage in the technical development of the RF probes with three prongs and their maximal deployment to a depth of 3 cm has not been tested at this time on any tissue volume-providing model. The significant aspect of the porcine liver anatomy is related to the volume of the blood perfused through the liver parenchyma per minute. While human liver perfusion rate is higher in males than females, measured at 115 – 125cc/100gm/min and 100 – 115cc/100gm/min respectively, and are food intake dependent. The swine liver flow is even higher. It may reach maximal flow rates during the postprandial period of up to 150 – 175cc/100gm/min. The volumes of blood perfusion play a significant role in the even distribution of RF energy through the organ parenchyma as demonstrated by previous animal experiments and by bench models [63].

The anatomy of porcine liver is similar to human liver in many aspects, however it is different in the allocation and composition of the liver segments. In contrast to the human liver, porcine segments lack lobar approximation and most of the segmental surfaces are covered by liver capsule. This aspect contributes to a slightly smaller volume of available liver parenchyma for ablation. This problem was overcome by the selection of domestic swine (sus domesticus) with body weight between20 – 30 kilograms. At this weight the size of the liver was large enough to accommodate the RF probe with full deployment of the prongs in all experimental groups

Twenty-eight domestic swine underwent radiofrequency ablation. The animals' care was delivered by the members of staff of the Animal Care Facility at Jack Bell Research Centre. The clinical and psychological care was provided according to the current facility protocol. The body weight, temperature, heart rate and behavioral observations were recorded daily.

2.1.2 Anaesthesia

All the animals underwent endotracheal intubation after intramuscular injection of Ketamine at a dose of 20 mg/kilogram. The anaesthesia was continued with isoflurane gas at 1.5% - 2% throughout the operation. After the surgery was completed the animals initially recovered in the post-operative room for 1 – 2 days in individual stations. The rest of the care was conducted after the animals returned to the group stations and were in direct contact with other experimental animals to improve to social quality of their life.

2.1.3 Analgesia.

The initial analgesia was delivered in the form of Bupenorphine at 0.01 mg/kg intramuscular injection every 12 hours. The requirements were based on an evaluation of animal appetite, respiratory rate and mobility.

2.1.4 The antibiotic therapy.

All animals were given antibiotic prophylaxis with Depocillin at 40,000 units/kg by intramuscular injection. Any possible post-operative infection would be treated with antibiotics of choice after either blood sample culture or wound discharge culture and antibiotic sensitivity were obtained.

2.1.5 The euthanasia.

Euthanasia was performed on day 30 after direct US examination of the right lobe lesion according to the Research Centre euthanasia protocol.

2.2 Radiofrequency equipment

2.2.1 Probe

The 15-gauge, triple electrode was used for all experiments (model RITA 3.1) (Fig. 3). All the probes and generator were provided by RITA Medical Systems, Mountain View, California, USA. Three hook-shaped retractable electrodes were deployable to a maximum diameter of 3.0 cm. The probe is insulated to within one centimetre of the tip to prevent cauterization along the shaft. Each electrode tip contains a thermistor that provides the temperature monitoring in the tissue immediately around the needle tip (accuracy $^{+}/_{-}$ 2°C from 35 – 100°C, and $^{+}/_{-}$ 5°C over 100°C) (Fig. 4b).

2.2.2 Generator

The radiofrequency generator (RITA Medical Systems) delivers a 460 KHz continuous unmodulated sinusoidal waveform in the bipolar output mode to a maximum of 30 Watts, which is optimized for desiccation. A generator with a maximum power output of 50 Watts was used for the animals in PGX group (Fig. 4a).

2.2.3 Data collection unit

During all RFA treatments data was collected in real time input directly from the RF probe and generator to a computer. The thermistor temperatures on each electrode, impedance, and delivered power were all recorded at 30-second intervals. During each of the experiments, the temperatures were monitored in real-time via time-sequenced graphs displayed on the computer monitor. All data was collected and evaluated with SPSS 10 for Windows. The independent variable t-student test and chi^2 or Fischer exact (for small samples) tests were used to compare the study groups. Both the electric parameters of the RF ablation and results of ultrasound examinations were evaluated for all the groups. The statistical difference was considered significant at $p<0.05$.

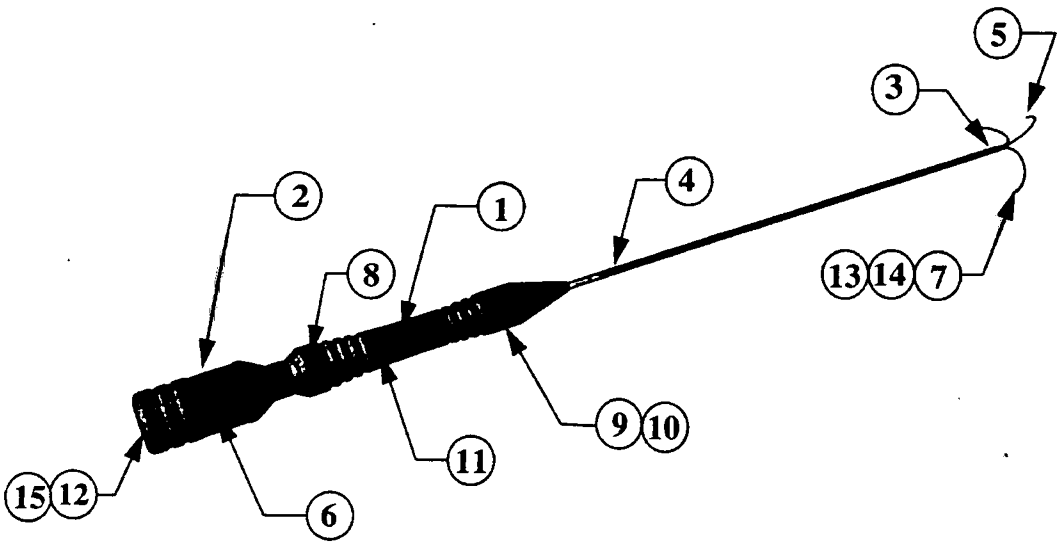

Figure 3. RITA model 30 Rev 3.2 (non-magnetic) radiofrequency electrode.

Materials list:

1. Main handle	PVC
2. Sliding handle	ABS
3. Main electrode	nickel-titanium
4. Main electrode insulation	polyester heat-shrink tube
5. Secondary electrodes	nickel-titanium
6. Internal RF wire	copper
7. Internal thermocouple	copper/constantan
8. Set screw	brass
9. Main electrode anchor	ABS
10. Main electrode anchor adhesive	epoxy
11. Secondary electrodes anchor	brass
12. Connector	bronze/copper/nickel/gold
13. Thermocouple insulator	polyimide
14. Thermocouple insulator adhesive	cyanoacrylate
15. Solder	tin/silver

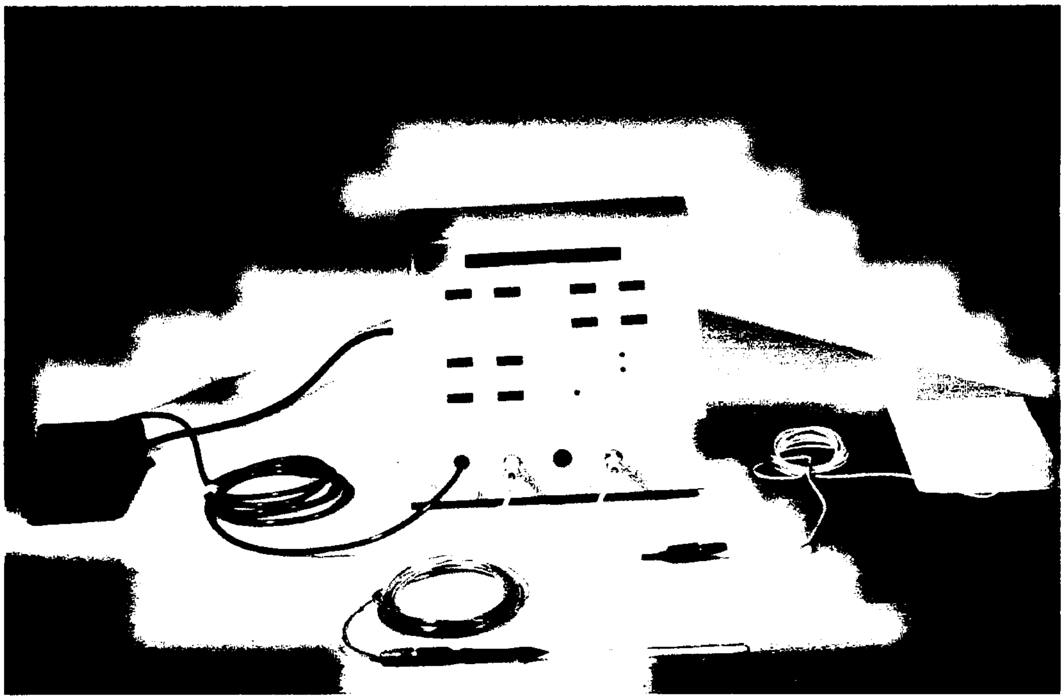

Figure 4. a) The generator unit with grounding pad, control pedal, and RF electrode.

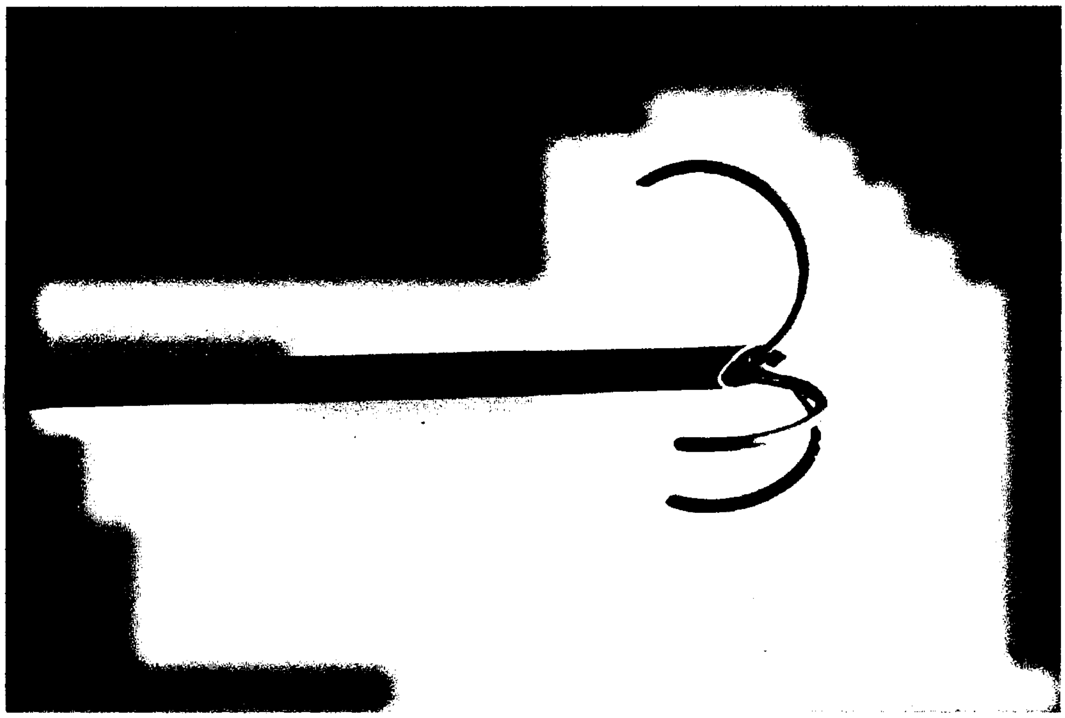

Figure 4. b) The enlargement of the electrode triple prong tip.

2.3 Experiment design

The study was designed in a precise way to anticipate any possible damage, which could happen due to application of RF within the liver parenchyma. The scenarios considered included an incorrect placement of the probe as well as unusual modes of the current delivery. The initial step included establishment of the predictable tissue ablation and consisted of the series of liver RF ablations with different common temperatures and subsequent examination of the liver parenchyma. This phase indicated a choice of a minimum temperature of 70°C on all the prongs in order to provide a consistently effective tissue ablation.

2.3.1 Preliminary phase

Three groups of 10 RF ablations, each at common temperature of: 50°C, 60°C, 70°C were performed. The tissue specimens underwent gross examination and comparison of ablation size and consistency of RF effect. The identified lesions were evaluated according to factors specified below:

-frequency of red area,

-frequency of white area,

-frequency of confluence of white area,

-size of the ablative tissue confluence area.

2.3.2 Main experiments

2.3.2.1 Experimental groups:

Anticipated complications were divided into four separate experimental groups:

1. Hepatic vein injury
2. Portal vein and bile duct injury
3. Diaphragmatic injury
4. Over exposure to RF energy (maximal application of RF energy)

***Experiment group 1* (PGA):**

Title: Hepatic vein injury secondary to RF

Purpose: To define potential injury to major veins due to direct approximation of the probe during the procedure.

Localization of the RF probe: 1 cm away from the confluence of main hepatic veins and IVC, with the tip of at least one prong 1 mm away from the wall of main hepatic vein or its major branch.

***Experiment group 2* (PGB):**

Title: Portal vein and major bile duct injury due to RFA

Purpose: To define potential injury to the major branches of the portal vein or main bile ducts due to RFA. These two structures were combined in one experiment, as their natural proximity was dictated by the anatomy of the porcine liver.

Location of the RF probe: visceral surface of the left and right liver lobe, 1 – 2 cm away from portal vein bifurcation.

Experiment 3 **(PGD):**

Title: Diaphragmatic injury due to RF ablation.

Purpose: to define potential diaphragm injury due to extracapsular or subcapsular application of RF energy.

Location of the RF probe: Left lobe – subcapsular placement (graph), right lobe – one prong extracapsular with tip of the prong in the diaphragmatic tissue (Fig. 5).

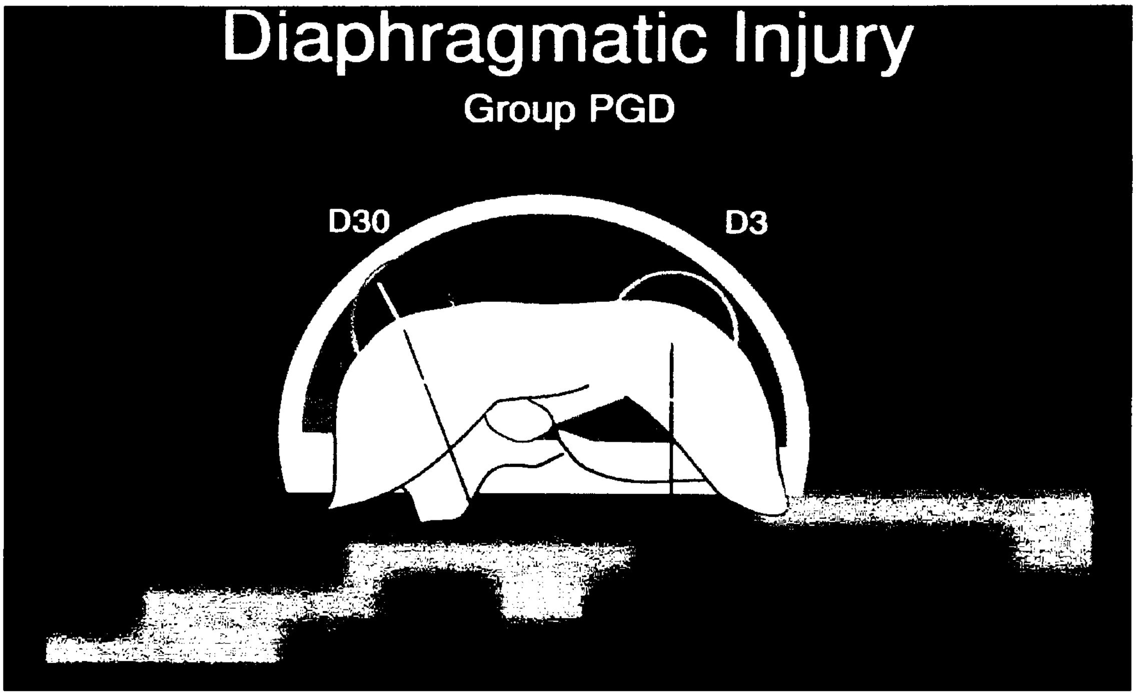

Figure 5. The graphic allocation of the RF probe placement in the diaphragmatic injury group. Day 3 (D3) position addresses the sphere of the RF energy between the prongs, while the day 30 (D30) position reflects the direct prong opposition of the RF electrode against the dome of the diaphragm.

Experiment 4 **(PGX):**

Title: Hepatic parenchymal injury due to RF overexposure.

Purpose: to define extent of possible liver injury due to over treatment with RF (temp 100 – 120°C).

Location of the RF probe: right lobe US guided placement and day 30 US exam only.

2.3.2.2 Experimental phases

The experiments in each group were performed in 3 specified phases:

1. Phase 1: Day 0 - laparotomy and RF ablation under US guidance
2. Phase 2: Day 3 - repeat laparotomy
   - US exam
   - Left segmental resection of the ablated liver
3. Phase 3: Day 30 - repeat laparotomy
   - US exam
   - Sacrificing of animal

Phase 1 **(Day 0):**

1. Animal anaesthesia and midline laparotomy
2. Direct access to the liver and US exam of treatment area of the left lobe
3. US guided RF probe placement with its prongs 1 mm from left hepatic vein wall or its major segmental branch. This was identified as 'day 3' tissue sample and model for the acute changes at its peak inflammatory response.
4. US guided RF probe placement in the right liver lobe in the similar pattern as above.
5. The RF energy application for at least 7 – 10 minutes to achieve the common temperature of 70 C.
6. Abdominal closure with running suture. End of anesthesia and extubation of the animal.

Phase 2 **(Day 3):**

1. Repeated laparotomy under general anaesthesia.
2. US exam and identification of the RF induced lesions in both lobes.
3. Left segmental liver resection.
4. Abdominal closure with one 'hemovac' drain and extubation.
5. Histopathologic evaluation of the day 3 specimen.

Phase 3 **(Day 30):**

1. Repeated laparotomy under general anaesthesia.
2. US evaluation of the Day 30 lesion in the right lobe.
3. Animal euthanasia and right lobe specimen provided for histologic exam.

2.3.2.3 Histopathology examination

The histological examination consisted of gross, hematoxylin and eosin (H+E) and histochemical NADH staining with light microscopic evaluation of the collected tissue samples on day 3 and day 30. The characteristics of the tissue were assessed to identify the pattern of tissue changes and possible interstitial complications. The NADH stain samples were used to confirm areas of tissue loss of viability and to provide precise definition of the lesion's edge.

All four experimental groups were assessed according to the acute and chronic phase of the RF induced interstitial injury:

1. Acute injury to the tissue and the vein – day 3
2. Chronic injury and resolution of acute changes to the tissue and the vein – day 30

2.3.2.4 Imaging studies

The placement of the RF probe during each of the experiments was guided by real-time ultrasound. The vascular identification and anatomy were conducted by Doppler phase ultrasound examination. The RF ablation lesions were followed up on day 3 and day 30 with ultrasound examination as well. The measurement of the lesions was performed with help of the clinical radiologist Dr. David Scallion. The US exams were performed in the routine way with identifying the lesion as containing characteristic echogenic "speckles" especially around the prongs and the main electrode shaft. The edges of the lesion had to be present with a sharp change of the echogenic image to be measured. The exam was performed in most of the cases by a team of radiologist and surgeon performing the laparotomy. Unless both investigators agreed on the quality of the image there was no measurement accepted as a valid US reading. All exams and measurements were conducted with Toshiba US Model SSH-148 and 3.75 MHz transducer covered with sterile cuff.

2.4 Histopathology

2.4.1 Gross examination

The gross pathology exam was performed in the standardized way. The Day 3 lesions were measured in the longitudinal axis and then sectioned along the long axis. The different zones of the ablation area where identified and described. Representative sections were selected for farther histologic examination by hematoxylin and eosin as well as histochemical NADH staining.

2.4.2 Hematoxylin and eosin (H+E) staining

Basic technique of staining of the tissue cellular structure was applied according to the protocol at the Department of Pathology and Laboratory Medicine at University of British Columbia, Vancouver General Hospital. Hematoxylin was used as a nuclear stain and eosin as the cytoplasmic stain. Cryostat frozen sections of liver tissue were cut at a thickness of 6 microns. Without fixation they were stained using following procedure:

1 minute immersion in Gill's hematoxylin (7%)

10 seconds water wash

10 seconds wash in 15% Sodium bicarbonate

10 seconds water wash

1 minute immersion in 3% aqueous eosin

20 seconds 95% ethyl alcohol wash

20 seconds 100% ethyl alcohol wash

20 seconds xylol immersion

Slides were coverslipped using "Entellan" mounting medium.

The results were the standard staining of the ablated and non-ablated liver tissue:

Nuclei - blue

Calcium deposits and cartilage – dark blue

Cytoplasm and other tissue constituents – varying shades of red

Blood – bright red

2.4.3 NADH staining

The histochemical examination with NADH methodology was selected for its efficiency in capturing necrotic changes or the degree of enzymatic preservation in damaged tissue. It also is named NADPH diaphorase as a reflection of the enzymatic properties of flavoprotein enzymes. These enzymes are involved in NADH hydrogen metabolism, and are the first ones to be destroyed when the process of tissue necrosis occurs. The response is independent of the injury mechanism. The method depends on the transference of hydrogen from reduced nicotinamide adenine dinuclaotide (NADH) and reduced reduced nicotinamide adenine dinuclaotide phosphate (NADPH) to a tetrazolium compound. The hydrogen transfer reduces the tetrazolium to produce a colored compound (black). Usualy tetrazolium compounds function as a hydrogen acceptor when diaphorases are being demonstrated histochemically, and the product of the reduction is the water-insoluble formazan pigment.

Tissue samples were cut in a cryostat as frozen sections at 6 microns in thickness. The results of tetrazolium staining are dependent on the tissue type, and its metabolic activity. Diaphragmatic muscle and hepatocytes both stain intensively. Cancer cells generally stain with less intense colour retention, because they have less metabolic activity. On the other hand necrotic tissues (ablation) do not stain with this method as the enzymatic processes within the cells are destroyed by thermal protein coagulation.

The stock tetrazolium solution consists of: MTT (1mg/ml) at 2.5 ml, hydroxymethyl aminomethane (TRIS) buffer at 2.5 ml, 0.5 M Cobalt Chloride at 0.5 ml, 0.05 M Magnesium Chloride at 1.0 ml, distilled water at 2.5 ml all adjusted to pH 7.0 using TRIS and NHCL. Incubating medium consists of stock tetrazolium solution at 0.9 ml, distilled water 0.1 ml, NADH 0.1 ml, adjusted to pH 7.1 and total volume of 2.0 ml. Unfixed frozen sections of tissue were immersed in incubating media at 37°C for 30 – 40 minutes. After incubation the slides were washed in the tap water for 5 minutes. Hematoxylin was applied as a nuclear counterstain for 1 minute. Finally water washing was performed for the 5 minutes. The processed slides were mounted in glycerine jelly and coverslipped.

CHAPTER THREE

3. RESULTS

All the experiments were completed according to the study protocol. The main thesis objective regarding the safety of radiofrequency ablation of liver parenchyma was answered. The current technology provides a good means to create volume ablation of liver tissue in different positions of the probe. The technique is simple and overall is safe. The tissue responds with a predictable pattern of injury and resolution, which does not create any long-term side effects for the treated animal. All the results may be considered as relevant to RF application in human liver.

3.1 Clinical outcome of RFA

Twenty eight female domestic pigs were used in the study. Out of this 26 were used for statistical analysis. There were no deaths related to uncontrolled or misplaced ablations. However, there were three animals, which died during the duration of the study. The causes of the death were as follows: 003PGB was euthanized immediately after the experiment for pain reasons as she suffered extensive 3rd degree burns to her back from a faulty non-insulated heatting pad and major facility power surges during the procedure, 006PGB died on day 6 due to undiagnosed bowel obstruction (autopsy confirmed volvulus of the stomach related to adhesions), 007PGB died at the end of the initial procedure due to cardiac failure (over sedation was suspected but the toxicology tests were not performed). The remaining animals did very well. Only two animals developed localized abdominal wound infections and required wound cleaning and additional antibiotics. The animals recovered from these infections without any health sequelae.

Overall the animals did exceedingly well taking into the account that all had to undergo two laparotomies and one segmental liver resection.

3.2 Initial minimal effective temperature experiment

During creation of the ablation was the initial changes occurred close to the prong and then extended away from the prong. Initial change was in the form of reddened area, which with passing time of experiment became area of palor. When the effective temperature was reached the areas around single prongs would become a confluent and slowly would extend to create the spherical shape. Because of these observations the assessment in this preliminary experiment was focused on three elements:

Presence and number of coagulative necrosis areas around individual prongs,

Presence of the 'reddening' area around each prong,

Presence of the 'white' (pallor) area around each prong,

Presence of confluence of individual prong ablation, and

Size of the area of confluence.

All the RF ablations were conducted in the same fashion. The tissue placement was guided by US and away from major liver structures like bile ducts, hepatic veins or major branches of portal vein. After the tissue placement current was delivered to the tissue and the experiment time of 7 minutes was measured from the moment when temperatures on all thermistors reached the group target temperature 50°C, 60°C or 70°C. Then the tissue samples containing whole ablated area were evaluated during gross pathology exam following the above criteria. 10 RF ablations were performed in each temperature group.

Evaluation of the minimal effective common temperature established that in the group with 50^{o}C as common temperature reached on three prongs for 7 minutes there was no volume ablation created in any of the samples. The mean number of the 'reddening' areas per experiment was 1.5 (SD 0.7). The mean frequency of 'white' areas was 0.4 (SD 0.7). There was no confluence of the white areas in any of the cases.

In the group with 60^{o}C only small amounts of coagulative necrosis were achieved and these were usually located around the prongs. The frequency of the 'reddening' area was at 2.2 (SD 0.8) and the 'white' area frequency was 1.8 (SD 0.9), and as in the previous group there were no cases of the 'white' areas confluences.

All the experiments in the group with 70^{o}C as common temperature were successful in creating grossly measurable ablations. The 'reddening' area was present at each of the prongs 2.9 (SD 0.3). The 'white' area was present around most of the prongs 2.7 (SD 0.4). This group was the only one to create consistent confluence of the prong related lesions, and the confluence was present in 70% of ablations, with the mean diameter of 2.7 cm (SD 0.4). The differences between the groups in all aspects of above evaluation were statistically significant with p value <0.001 (Fig. 5,6)(Table 1).

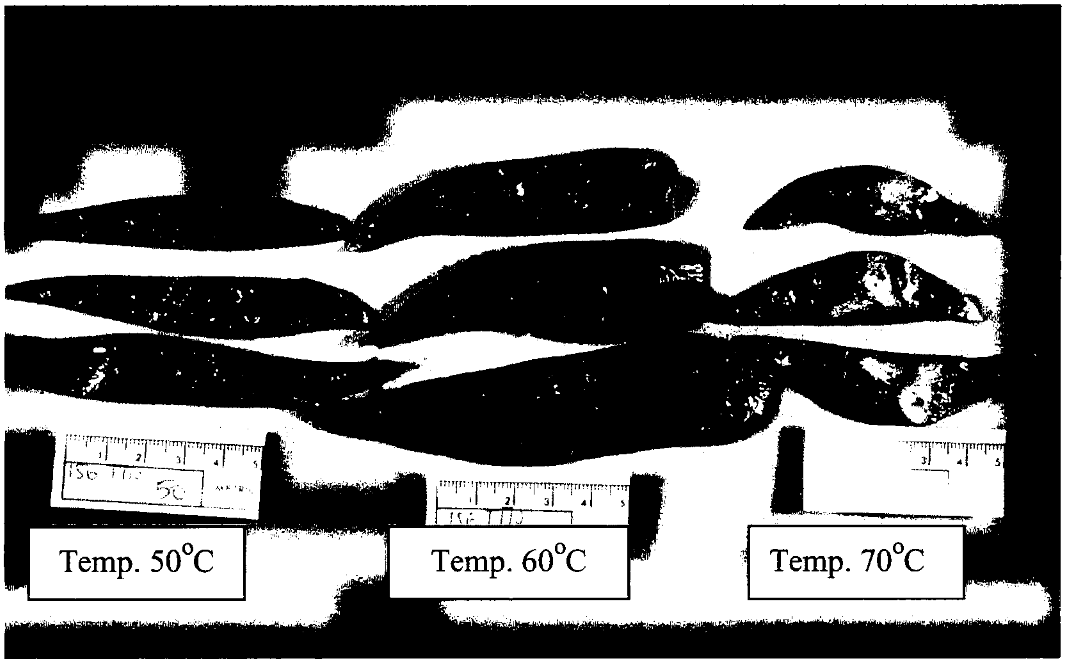

Figure 6. The gross pathology, the RF lesions created at different treatment temperature range, notice the confluence of the prong's ablations in the higher temperature range.

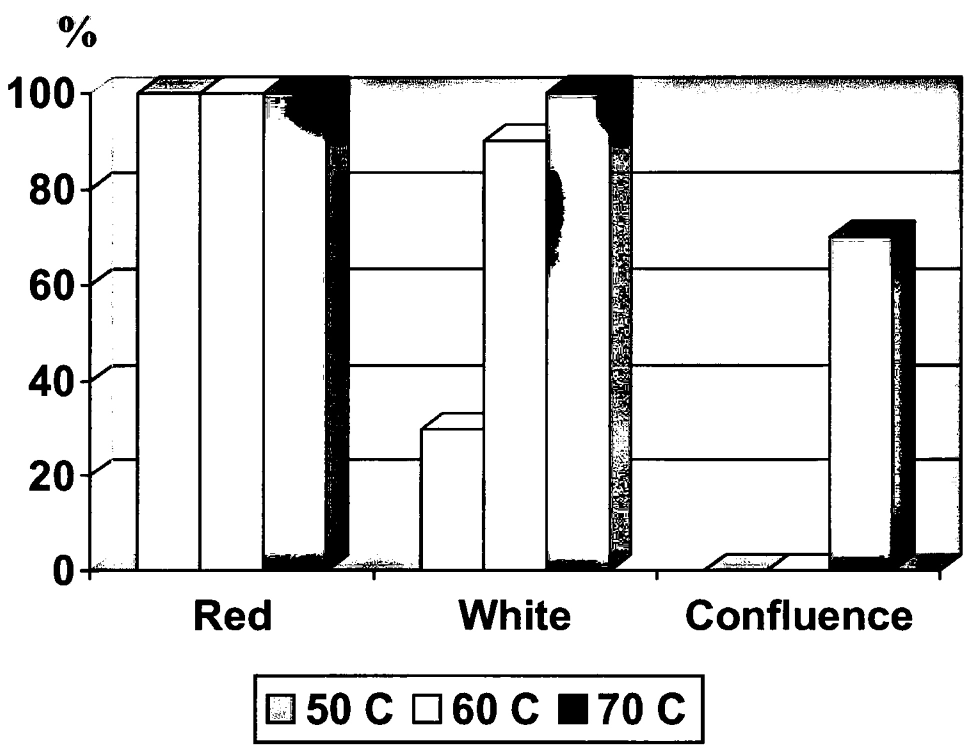

Figure 7. The frequency of 'reddening' area (red), 'white'area (white) and confluence of the ablation around the prongs (confluence) in the minimum effective treatment temperature groups at 50°C, 60°C, and 70°C (in %).

Temperature Group	N° of red areas Mean and (SD)	N° of white areas Mean and (SD)	Size of necrosis confluence (cm)
50°C	1.5 (0.7)	0.4 (0.7)	0
60°C	2.2 (0.8)	1.8 (0.9)	0
70°C	2.9 (0.3)	2.7 (0.4)	2.7 (0.4)
P value	<0.006	<0.001	<0.001

Table 1. The mean number of measurable lesions created by RF ablation in the preliminary phase defined by the minimum common treatment temperature and its effectiveness in reliable creation of the thermal injury.

3.3 Histopathology

The pathology exams were performed in the routine way with the assistance of consulting pathologist Dr. David Owen. The tissue samples were preserved for several days in 10% formalin solution before proceeding to microscopic examination with H+E staining and histochemistry for NADH activity.

The findings were overall similar in appearance among all groups and the observations will be presented for the whole study group.

3.3.1 Gross

The gross exam was conducted in several samples on day O and day 3 on fresh tissue. The samples were measured only in selected cases to assess the diameter of the RF lesion in its largest part. The gross observation revealed a fairly consistent pattern of the RF ablation regardless of the experimental group. The pathology findings were then grouped by the day of experiment. The results are presented according to the findings on each specified day.

Day 0:

Zone A: the central zone consists of mechanical defect occupied by the probe.

Zone B: most immediate tissue surrounding zone A consists of mechanically damage cells and stroma.

Zone C: grossly appearing as so called 'pale' zone has its tissue structure preserved with a pale-grey appearance.

Zone D: grossly described as a 'reddened' zone, appears red, edematous, and stiff up to the abrupt end of the ablation sphere (Fig. 8a).

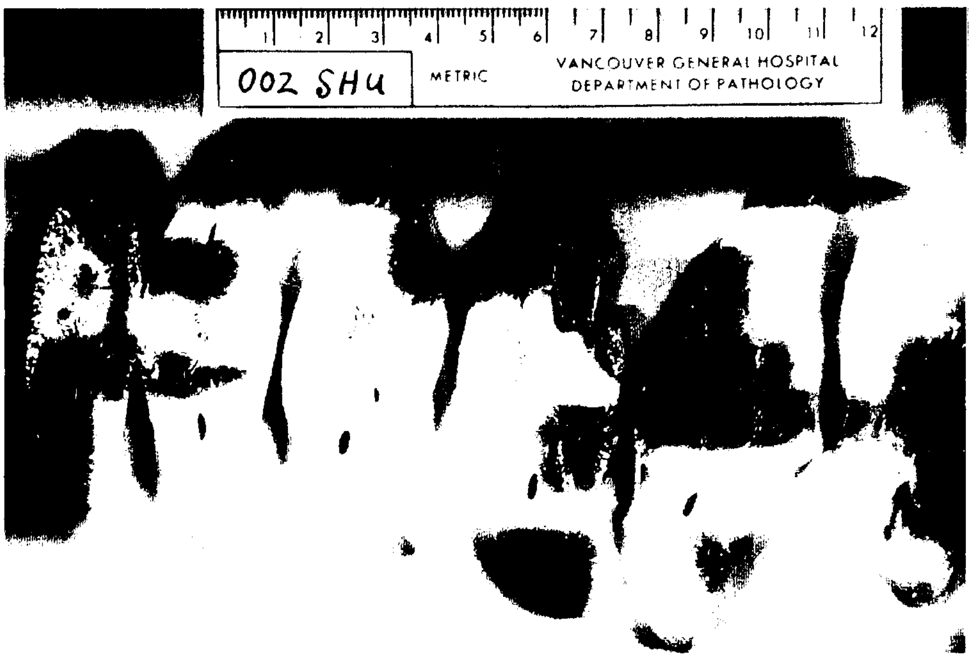

Figure 8(a). Gross pathology exam day 0 sample with the prominent zonation. The central mechanically damage zone is surrounded by 'pale' area and than 'red' area at the periphery of the ablation.

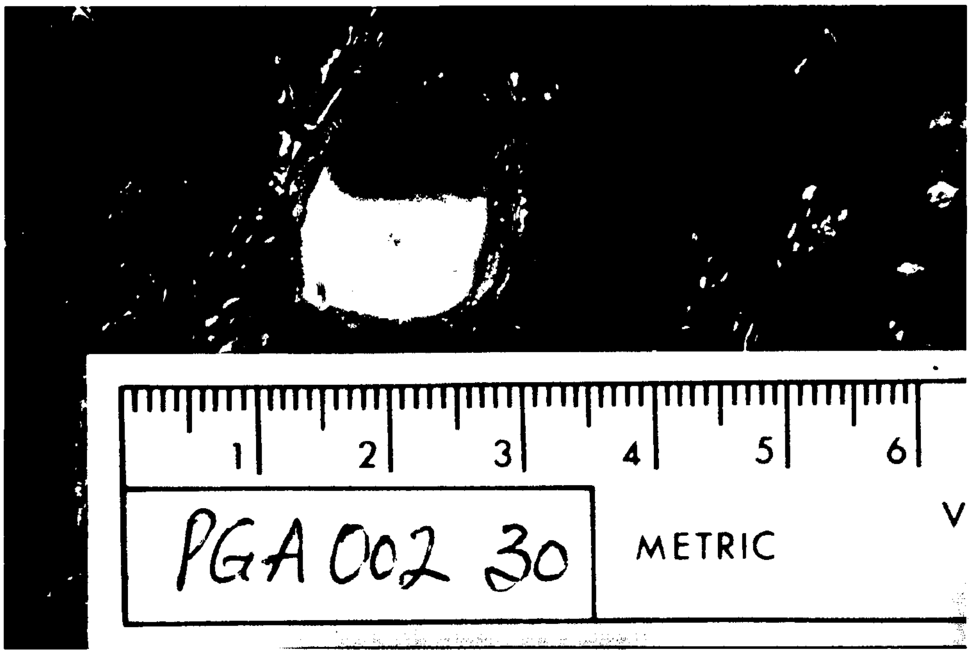

Figure 8(b). The day 30 changes show the homogenous necrotic tissue surrounded by the fibrous capsule.

Day 3:

The gross appearance of the tissue was somewhat similar to the day 0 findings. The zonification was less prominent and the tissue had the same early coagulative necrosis picture. The periphery of the RF lesion presented a sharp demarcation between the ablated tissue and normal liver tissue. There was no capsule formation at this stage. No obvious pathology like haemorrhage, hematoma, bile leak, or bile accumulation was identified.

Day 30:

The demarcation of the lesions was completed. There was a well formed capsule around the ablation measuring up to 1 mm thickness in some cases. Shrinkage of the lesions was present in variable degree from small to almost complete absorption. The previously present zonation was lost. There was no cyst or abscess formation present (Fig. 8,b). The vessels in most of the RF ablations were separated from the demarcated area by normal liver parenchyma (Fig. 9).

3.5.2 H+E

The findings were consistent in all the groups regardless of the targeted intrahepatic structures or the absorption of the current. The zones described in the above section had their representative features on H+E staining.

Day 0 microscopic findings consisted of:

Zone A: was lacking of any cellular structures, i.e. the needle tract

Zone B: showed no stained hepatocytes with moderate to severe interstitial destruction either in form of damaged cells or tissue separation, zone of tissue charring (Fig. 10a).

Zone C: the 'pale' area contained microscopically intact, however mildly edematous hepatocytes without staining or very light staining with H+E and vessels packed with empty appearing erythrocytes, which resembled ghost like structures. The hemoglobin, the main content of the erythrocyte cytoplasm was unable to retain the H+E stain. This would be consistent with total destruction and thermal denaturation of protein structures with cytoplasm (Fig. 10b).

Zone D: the 'reddened' zone had normal H+E staining with some degree of cellular edema and vessels distended with red stained erythrocytes. The erythrocytes were ballooned and gave the impression of packing the lumen of the small vessels, sinusoids very tightly (Fig 10c,d).

The periablation tissue stained in usual fashion with H+E. Local sinusoids contained normal amount of erythrocytes and the cells were not edematous.

The changes consistently observed on day 3 and 30 were similar in all the experimental groups. In general the changes may be grouped as follows:

Day 3:

The lesion still demonstrates some form of zonation, however the size and differentiation may be variable. The cells within the ablation appear more necrotic and present either kariolysis or karyorrhexis (Fig. 11a,b). The periphery of the ablation shows a very sharp demarcation, sharper than on day 0 (Fig. 11c). The surrounding liver parenchyma is populated with regenerating and proliferating hepatocytes. The inflammatory cells population was similar or smaller than on day 0.

Day 30:

The demarcation of the ablation was completed. A fibrous capsule was formed in all the samples. The thickness of the capsule was variable up to 1 mm. Inside the capsule the liver tissue was totally necrotic. The outlines of the heptocytes were lost, however aggregates of nuclear DNA were present. Overall the general basic tissue architecture was still preserved (Fig. 12).

3.5.3 NADH

The NADH staining was conducted only on limited number of tissue sample for confirmation purposes. The samples processed with NADH diaphorase proved that all the tissue within the RF ablation zone was dead at the time of completion of the ablation. The areas around some large vessels indicated on occasion there were small amount of tissue with the residual enzymatic activity. The edge of the ablation was always sharp and the border between the necrotic and normal viable liver tissue was in the range of one to two cell lines.

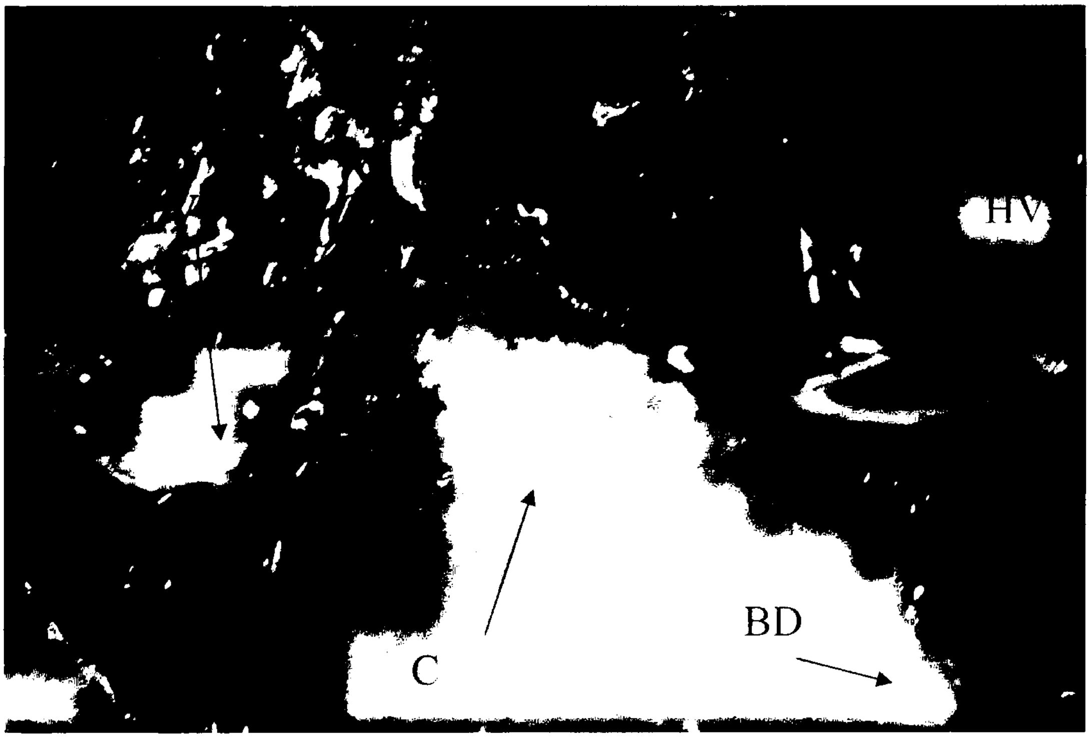

Figure 9. Day 30 gross pathology. The lesion is well contracted with a well defined capsule (C). The RF lesion is surrounded by hepatic veins (HV), portal vein branches (PV), and bile ducts (BD). All the structures look well preserved and functional.

Figure 10(a). Central part of the ablation, Zone A and B with mechanical tissue damage and complete destruction of the liver tissue in zone B.

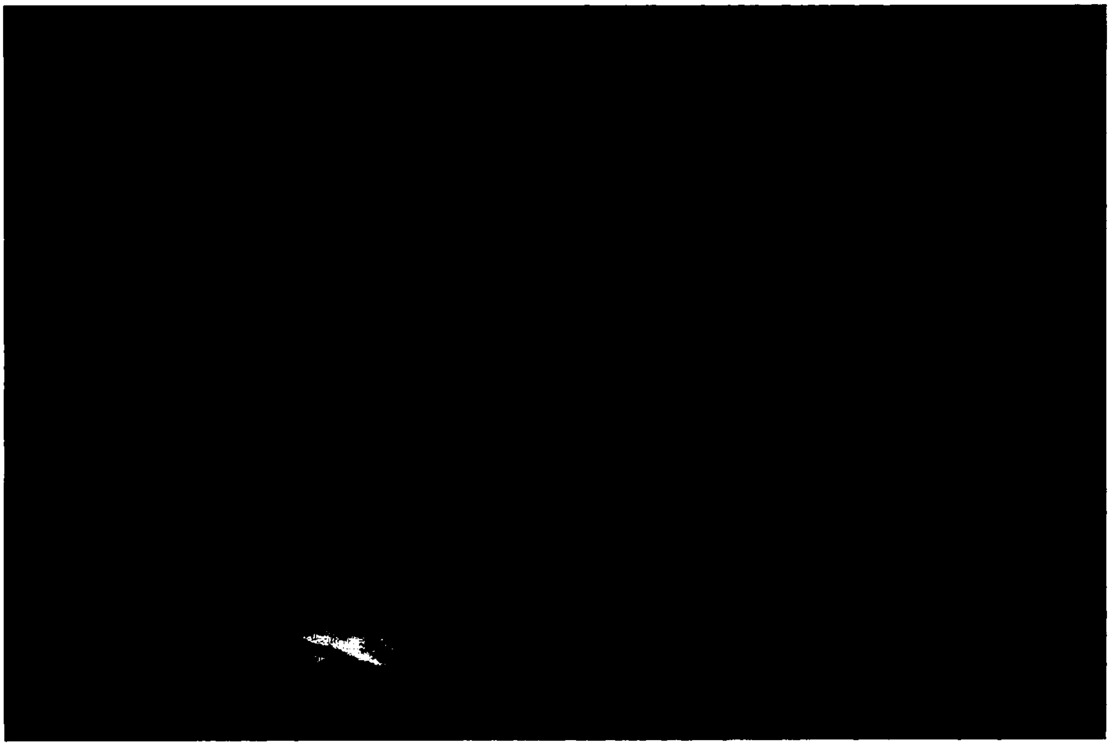

Figure 10(b). Zone C changes with preserved infrastructure of the liver tissue. Day 0 changes with empty erythrocytes and still staining nuclei.

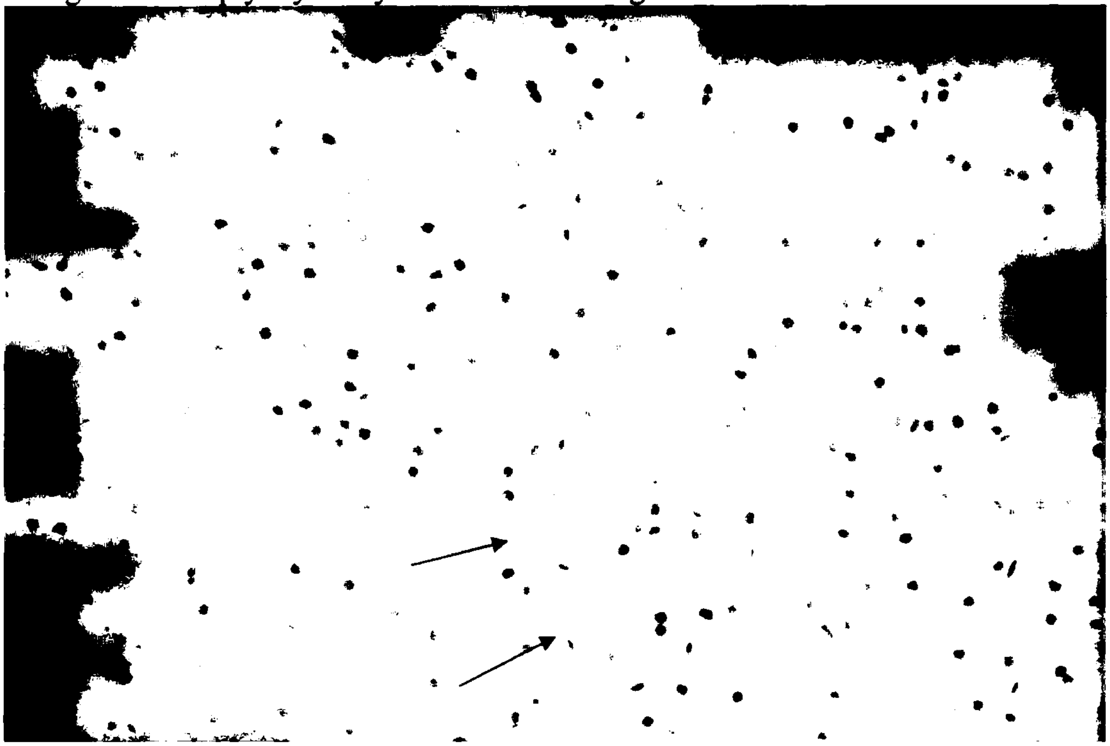

Figure 10(c). Zone C 100x enlargement with severe degree of cytoplasm coagulation (foamy cytoplasm) and H+E stain lacking erythrocytes obliterating sinuses (arrows).

Figure 10(d). Zone D with sinuses congested by H+E positive staining erythrocytes. Zone of "reddened' area.

Figure 11(a). Day 3 kariolysis in the RF ablated tissue.

Figure 11(b). Day 3 karyorrhexis in the RF ablated tissue.

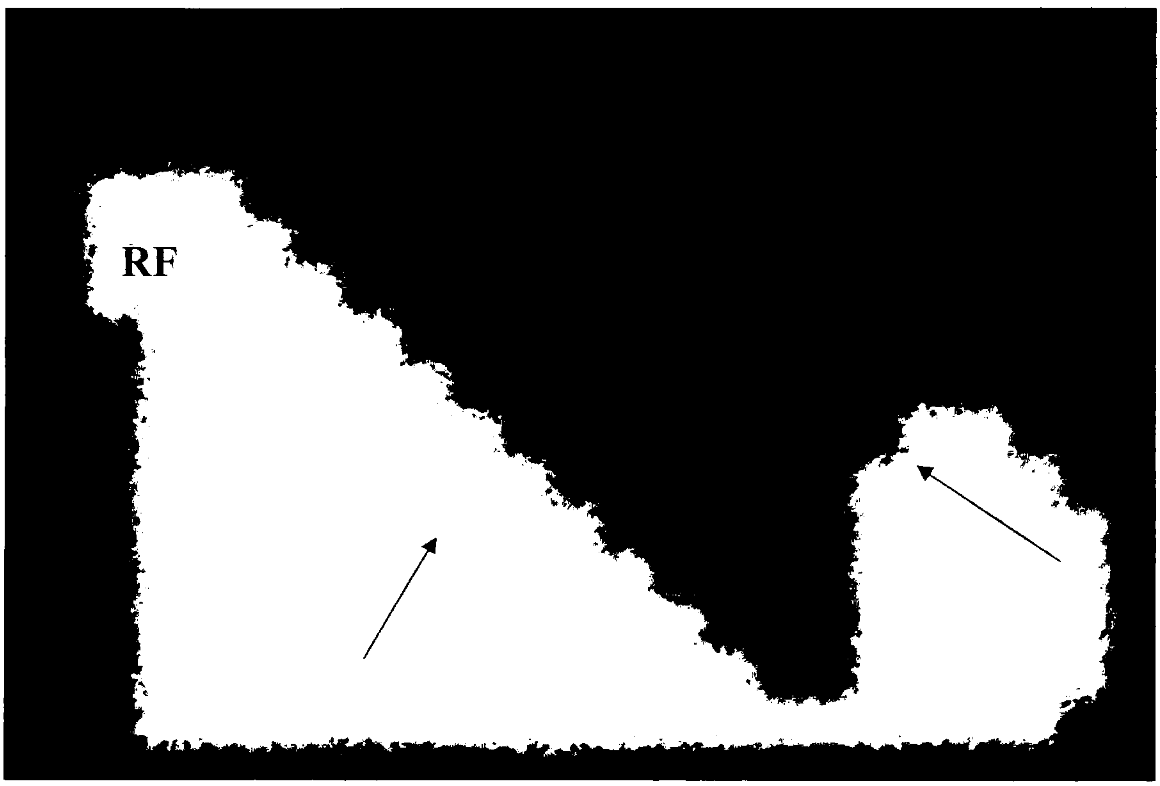

Figure 11(c). Sharp edge of the ablation periphery with normal alive liver tissue 1-2 cell width away from the RF ablated tissue.

Figure 12(a). The H+E staining of the day 30 liver tissue healing. The DNA remnants and faint preservation of the liver acinar anatomy.

Figure 12(b). The fibrous capsule and the edge of normal liver tissue present at the bottom of the picture on day 30 of the experiment.

3.4 Parameters of RF ablation

The data during RF ablation was collected in real-time with recording of the maximal power delivered to the tissue during the ablation, mean power throughout the procedure, total energy delivered to the ablation area and impedance of the tissue during the experiments. All the data was collected and evaluated for each experimental group. The results are presented in the table below. The shorter time of effective ablation in the PGA group is due to relatively small volume of the left lobe in the area where the probes were placed. This led to shorter period of time reaching the target common temperature on all the prongs at 70°C. The remaining groups required a longer time to reach the minimum required common temperature. (Table 2.)

	Experimental Groups			
	PGA (N=6)	**PGB** (N=8)	**PGD** (N=8)	**PGX** (N=6)
Length of experiment (min.)	10	15	15	15
Mean temperature above 70°C	6.5	8.8	11.8	13.5
Mean Power (Watts)	23.4	27.5	27.2	37
Mean energy delivered to the ablation area (joules)	14 898	25 622	25 730	34 262
Mean impedance (Ohms)	97.8	80.5	73	117.4

Table 2. Summary of the RF ablations in the different experimental groups.

3.4.1 PGA

The ablations in this group were performed close to the wall of the hepatic vein or its major branches (Fig. 13). The average time to achieve a grossly significant ablation for the whole group was 6.5 minutes of effective treatment temperature (ETT). The mean power delivered to the tissue was 23.4 Watts. Total energy delivered to the ablation area was a mean of 14 898 joules per ablation. The tissue impedance was fairly high at a mean of 97.8 Ohms for the whole group.

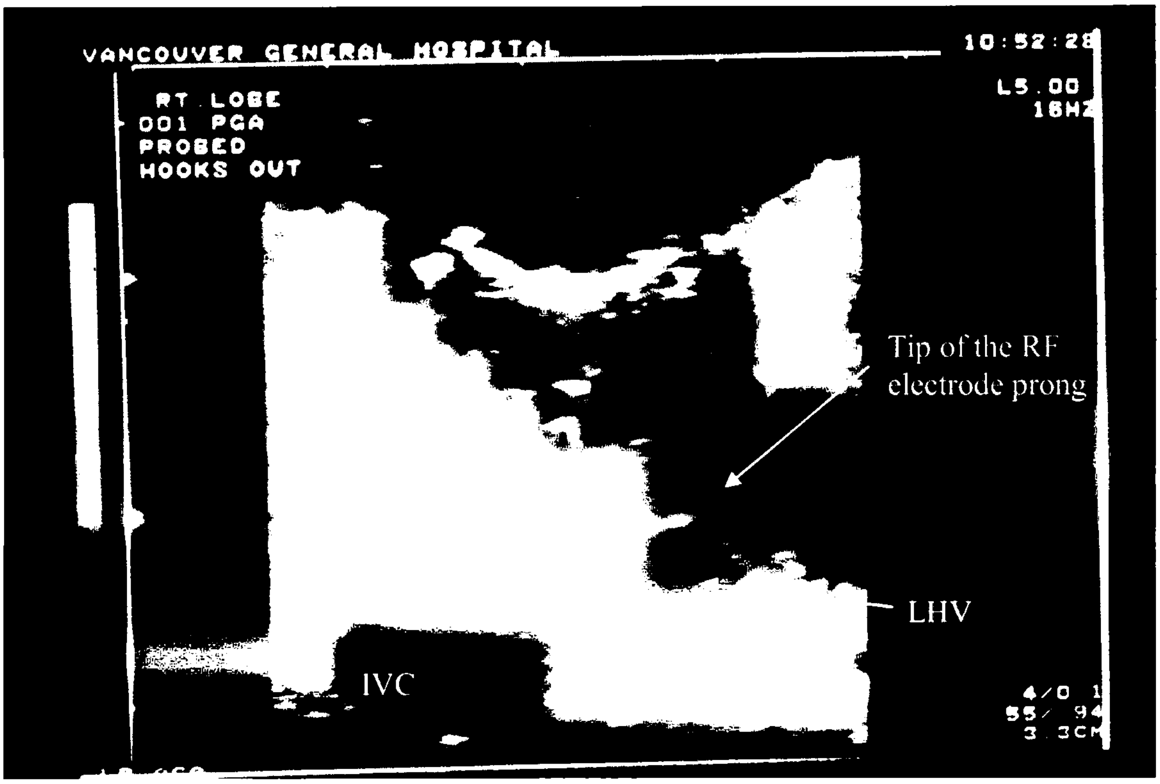

Figure 13. Ultrasound image of the RF electrode prong placement close to left hepatic vein wall (LHV), (IVC) inferior vena cava.

3.4.2 PGB

A total of 16 RF ablations were performed in the group with attempted bile duct and portal vein ablation. The mean time of experiment was 15 minutes, due to the need for longer current flow through the tissue in order to achieve a US recognizable image. The mean time of the effective treatment temperature (ETT) was 8.8 minutes. The mean power delivered to the tissue was 27.5 Watts. The mean amount of energy delivered to the tissue was 25,622.00 joules and the mean impedance was 80.5 Ohms.

3.4.3 PGD

A total of 14 ablations were performed in the diaphragmatic injury group. The mean experiment time was 15 minutes, while the mean duration of effective treatment temperature (ETT) was 11.8 minutes. The mean power delivered was 27.3 Watts. The mean amount of energy was 25,730.00 joules per treatment. The mean impedance was 73 Ohms. The ablations were successful and all left-sided (current sphere induced) and right-sided (direct prong induced) ablations resulted in the some degree of diaphragmatic burn injury.

3.4.4 PGX

In this group the ablations were performed only in the right liver, during percutaneous access. Successful RF ablations were created in six animals. The total experiment time was 15 minutes. The effective treatment temperature (ETT) was sustained for a mean of 13.5 minutes. The mean power delivered during the ablation was at 37 Watts. The mean amount of energy absorbed by the tissue was 34,262.00 joules. The mean impedance recorded for the group was 117.4 Ohms, the highest of all experimental groups.

3.5 Microscopic tissue changes and adaptation

In all the cases of RF ablation the liver tissue presented the same histologic picture of coagulative necrosis. The zonification of the lesions was consistent throughout all groups. Zone A consisted of a central space occupied by the shaft of the probe. Zone B, surrounding zone A, was very thin with mechanical destruction to the cellular structure and tissue charring. Zone C was named 'palor' (white) zone on gross exam and zone D, so called 'reddened' zone was most peripheral area of necrosis. The surrounding tissue appeared not to be damaged with very sharp (one or two cell width) transition to normal tissue.

The tetrazolium reaction confirmed that tissue necrosis extended to the outer margin of the reddened zone. The histologic difference between the reddened zone and palor zone simply reflected a difference in sinusoidal dilatation and erythrocyte congestion.

3.5.1 Vascular structures and high flow vessels

The ablation of the vessel containing tissue indicated some form of interaction between the small vessels and large volume vessels within the tissue. The vessels of small diameter were coagulated when within the area of RF ablation. The large vessels seemed to be preserved without any short or long-term sequellae. The peripheral positioned large flow vessels were the main reason for less than perfect shape of some of the ablations.

This phenomenon was observed in all the samples of the tissue regardless of the study group allocation. The vessel wall was either preserved or coagulated depending on the vessel size and distance from the centre of the RF ablation. In cases of some large vessels there was a very slim cuff of tissue preserved around the vessel. The wall of the vessel close to ablation did demonstrate inflammatory changes on day 3. Infiltration with inflammatory cells particularly neutrophils and tissue edema was obvious and locally very severe. The changes included all the layers of vascular wall from intima to adventitia. Even in the presence of intima injury there was no adherent thrombosis identified. Despite the substantial size of periportal vein adventitia, which is a continuation of portal plate stromal connective tissue, the portal vein injury demonstrated the same microscopic attributes as the hepatic vein wall injury. There was one example of infarct of Zahn in the PGB group (marked PGR) on day 30. An infarct of Zahn is described as segmental partial ischemia or hypoperfusion due to occlusion or thrombosis of one of the vessels supplying given area of liver that has a dual blood supply. The reduction in blood supply causes hepatocyte atrophy with compensatory sinusoidal dilatation. In this particular pig's liver there was resolving perivascular necrotic tissue in the initial stage of the scar formation (Fig. 14). There were no signs of haemorrhage or hematoma present in any of the tissue samples.

3.5.2 Bile duct related structures

Small size bile ducts were either totally ablated in the centre of the lesion or preserved on the periphery of the ablation. The stromal tissue present around and along the distribution of the biliary tree was coagulated to the same degree as the bile duct wall itself. There were no signs of bile duct rupture or bile duct leak in the specific group as well as in the whole experimental group. The incidence of interstitial bile collection, so called biloma, was zero.

3.5.3 Diaphragm

The diaphragm is a muscle and fibrous tissue dome like structure functioning as a part of ventilatory mechanism and a separation structure between the cavity of the chest and abdominal cavity. The left diaphragm injury lesions were created by the RF current sphere between the deployed prongs, and presented as tan area of erythema and edema on the day of RF ablation. However on day 30 the lesions were difficult to identify. The area was completely healed and fully functional. The lesions created in the right part of the diaphragm were actually due to direct opposition of the single prong against the diaphragm muscle. Remaining prongs were embedded in the liver parenchyma. The resolution of this type of injury was an almost complete re-absorption of the necrotic liver tissue and despite major thermal injury to the diaphragm muscle the full recovery of its structure. (Fig. 15). There was always a dense adhesion between the peritoneal surface of the diaphragm and liver capsule in the area of RF ablation.

3.4.4 Maximal energy application

The PGX RF ablations were evaluated only one time with pathology exam and it was on day 30. The animals survived these experiments without any clinical complications. The findings on histological examination were consistent with RF coagulative necrosis resolution pattern present in the previous groups. One complication in the group was present in the form of complex cyst. The histology proved this to be uninfected, non bile containing complex cyst (Fig. 16).

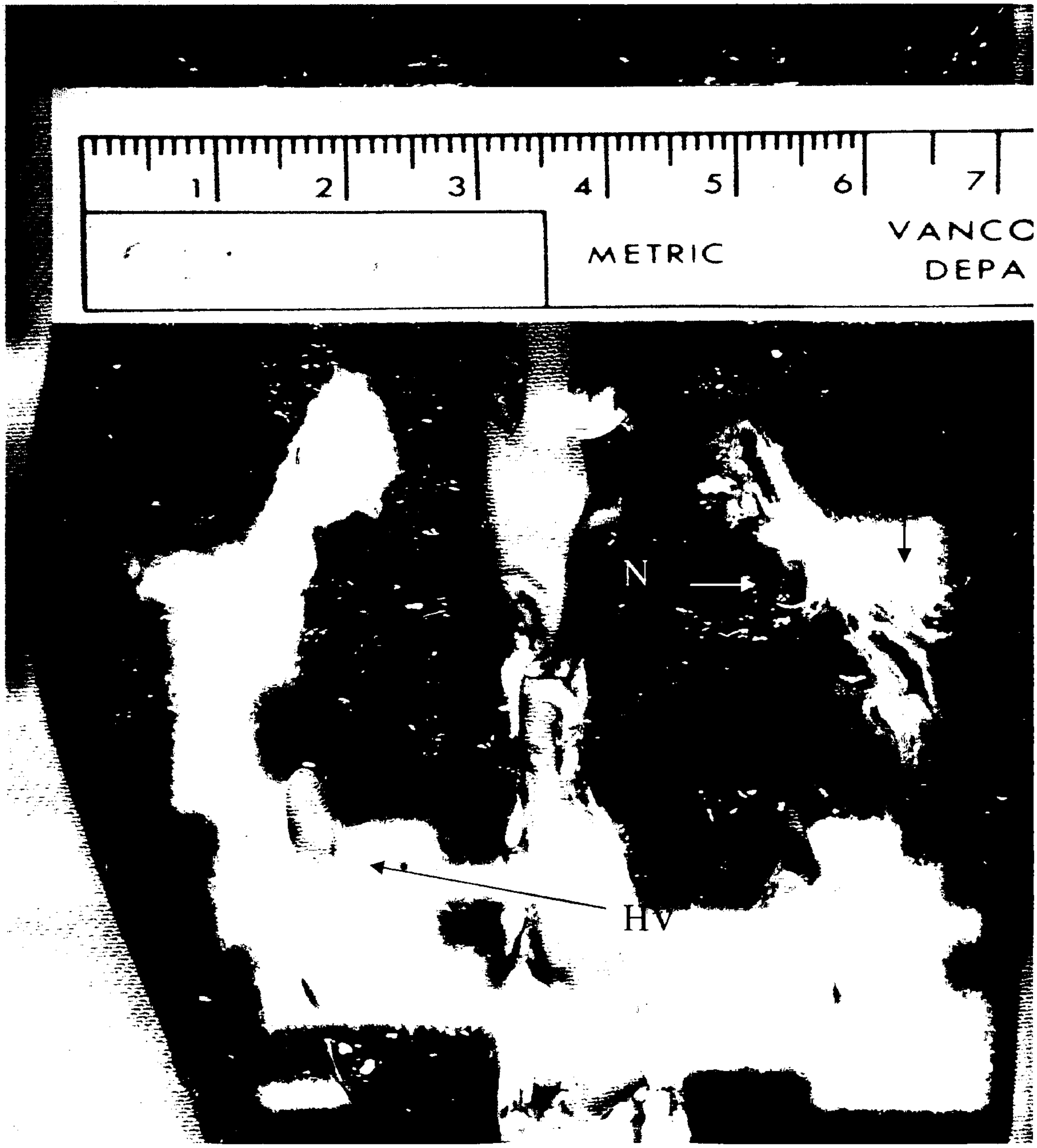

Figure 14. Infarct of Zahn (Z). The interruption in the proper blood supply to the segment of the liver presenting with lighter pink colour. The normal hepatic veins (HV) and dilated parts of the portal vein (PV) due to obstruction of the PV flow by RF necrosis resolution (N).

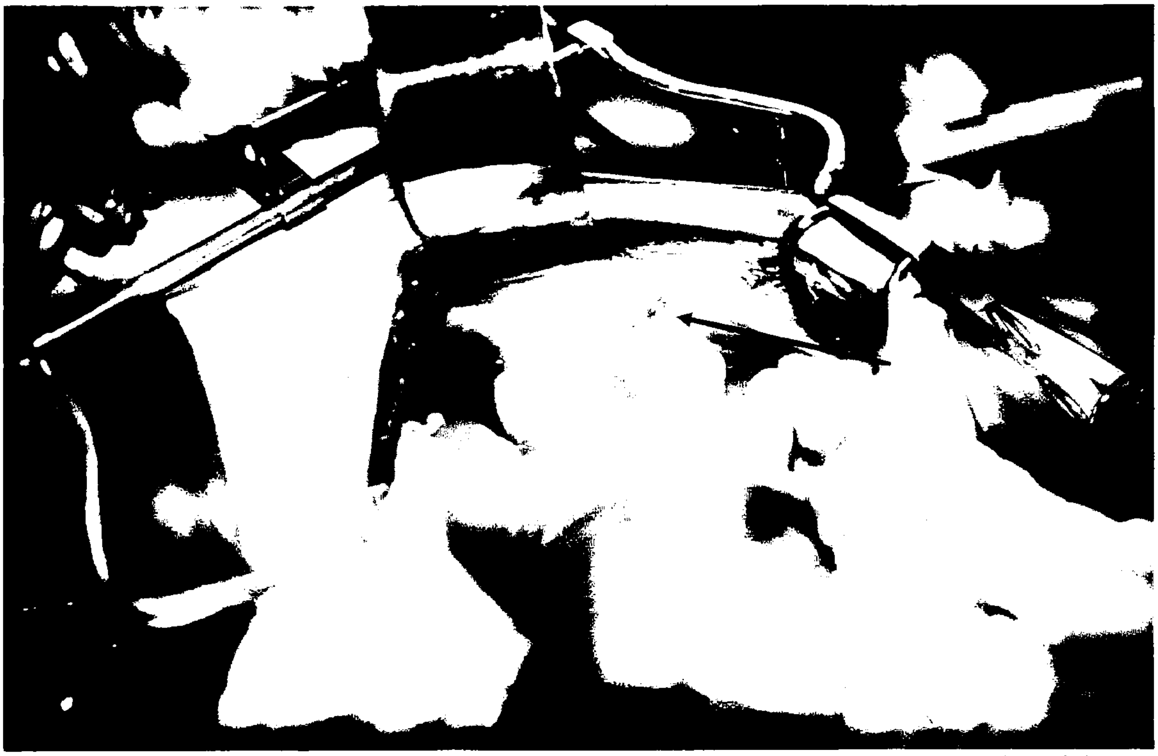

Figure 15(a). Day 3 diaphragmatic response to the RF ablation in the right lobe of the liver. The diaphragmatic 2-3° degree thermal burns (arrow).

Figure 15(b). Day 30 resolution of RF ablation to the diaphragm. The liver lesion follows the previously documented changes, while diaphragm appears completely healed.

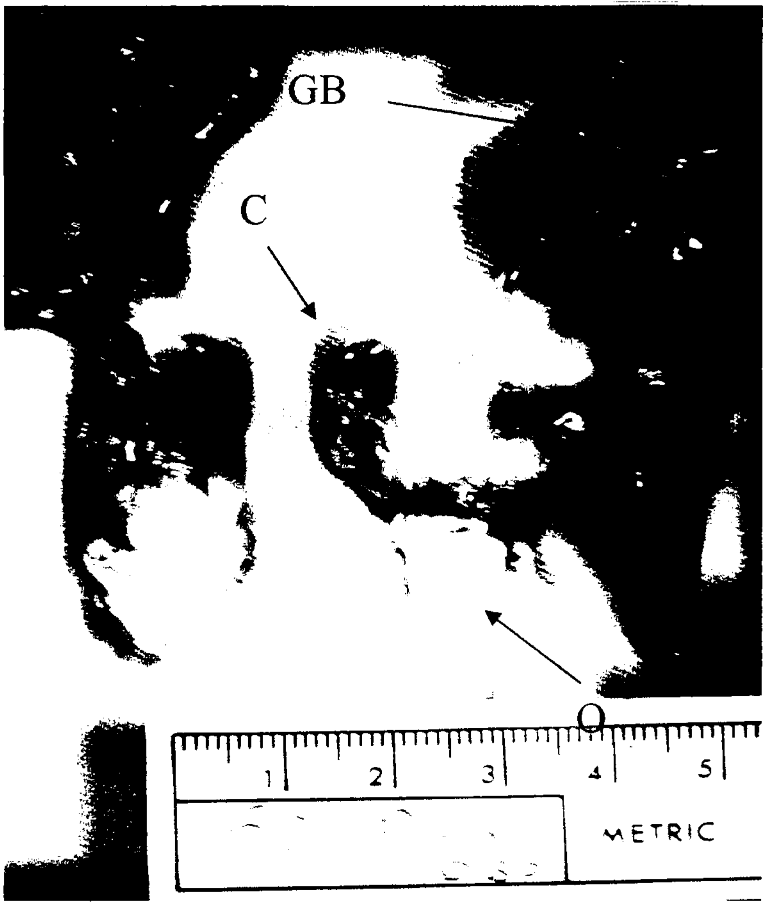

Figure 16(a). Resolution of the RF ablation in the PGX group. An example of possible outcome in the form of complex cyst (C) in the area close to the omentum (O) and gallbladder (GB).

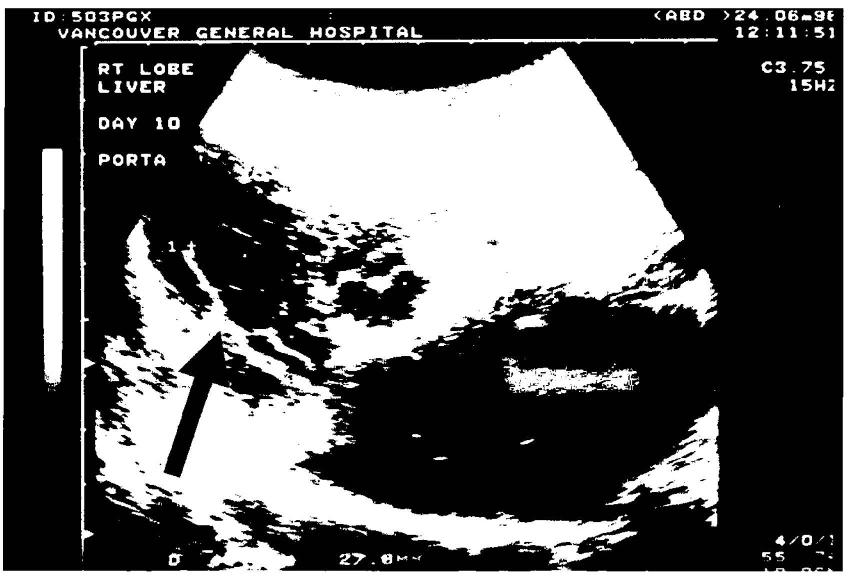

Figure 16(b). Ultrasound image of the complex cyst at day 10 (arrow).

3.6 Ultrasound technology

Evaluation by US was performed according to the phase of the study. The day 0 US imaging was considered as US guidance application, while the day 3 and 30 exams were evaluated for the merit of this imaging as a method of follow up. The previously described criteria had to be agreed upon to proceed with the recording of the lesion measurements. The Day 0 RF ablations in the PGD group were performed without US examination as the goal was primarily focused on the position of the prongs against the diaphragm, rather than creation of necrosis.

3.6.1 US as a RFA guidance

The evaluation of the probe position in the tissue and its relationship to intrahepatic structures like hepatic veins, portal vein branches and bile ducts was achieved without difficulties in all the cases. The assessment of the lesion's size in most cases on day 0 was uncertain and measurements were not recorded. The visual images did not show sharp enough borders to proceed with accurate measurement. The lesions themselves however were easily identifiable. The characteristic combination of "speckles" around the position of the prongs within each ablation was imaged in all cases.

3.6.2 US in follow up

The tissue changes in form of sharper edges, vacualisation of the periphery of the lesion and progressing necrosis produced a much more precise demarcation of the lesion on US exam. The efficacy was up to 75% in the group PGA and 100% in the group PGX on day 3 exam (Fig. 17a,b).

The changes in chronic phase on day 30 with complete demarcation of the lesion and some degree of the necrotic tissue shrinkage reduced the sensitivity of the US exam in this phase to 33% in the PGA group and 66% in the PGX group. Some of the lesion were undetectable by US due to their size and were only later identified on gross pathology exam.

The groups with the lowest measurability of the RF ablation lesions were the ones where the ablations are most difficult to guide and follow up. The high vascular areas like in the PGB group (portal vein branches and small arteries) and subcapsular hepatic ablations with prongs so superficial, that the organ's interfaces are adding to the diminished US sensitivity. Only several cases could be followed with successful US follow up throughout all the experimental phases. The imaging captured in this case was most well preserved liver tissue in the whole series (Fig. 18).

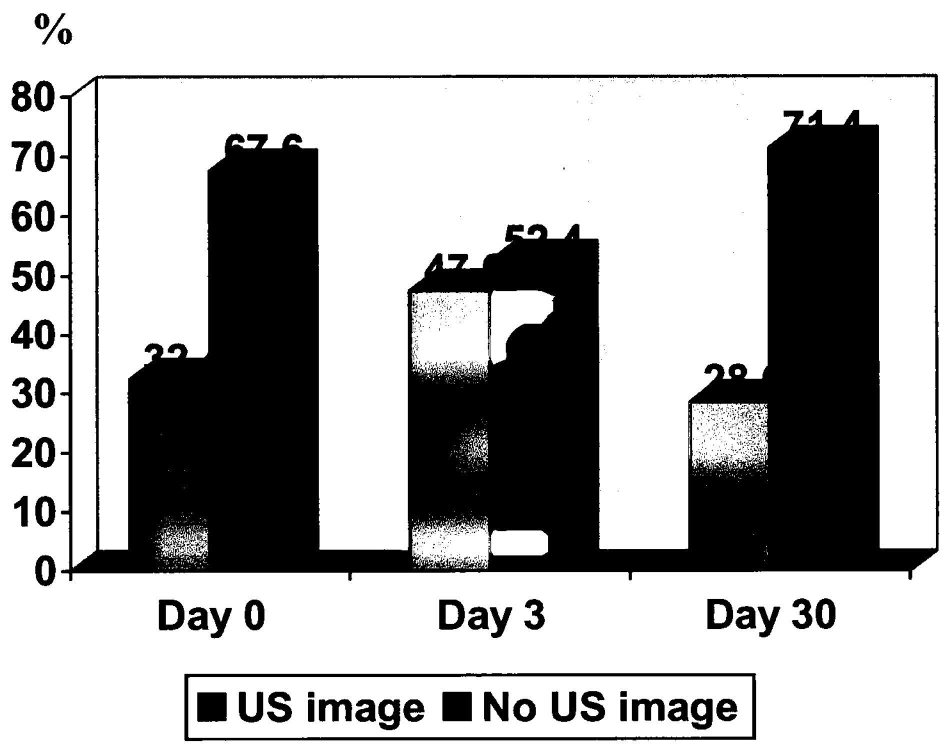

Figure 17(a). The US technology identifying the RF lesions was partially effective. The difference between the groups and the days was of no statistical significance (p=0.2).

Group	**Day of US exam**		
	Day 0	***Day 3***	***Day 30***
PGA	3/12	9/12	2/6
PGB	4/16	4/16	1/8
PGD	--	1/8	1/8
PGX	4/6	6/6	4/6
Total	11/ 34	20/42	8/28

Figure 17(b). The US exams performed during the study. Numbers represent the measurable lesions and total number of US exams in the group by the study phase.

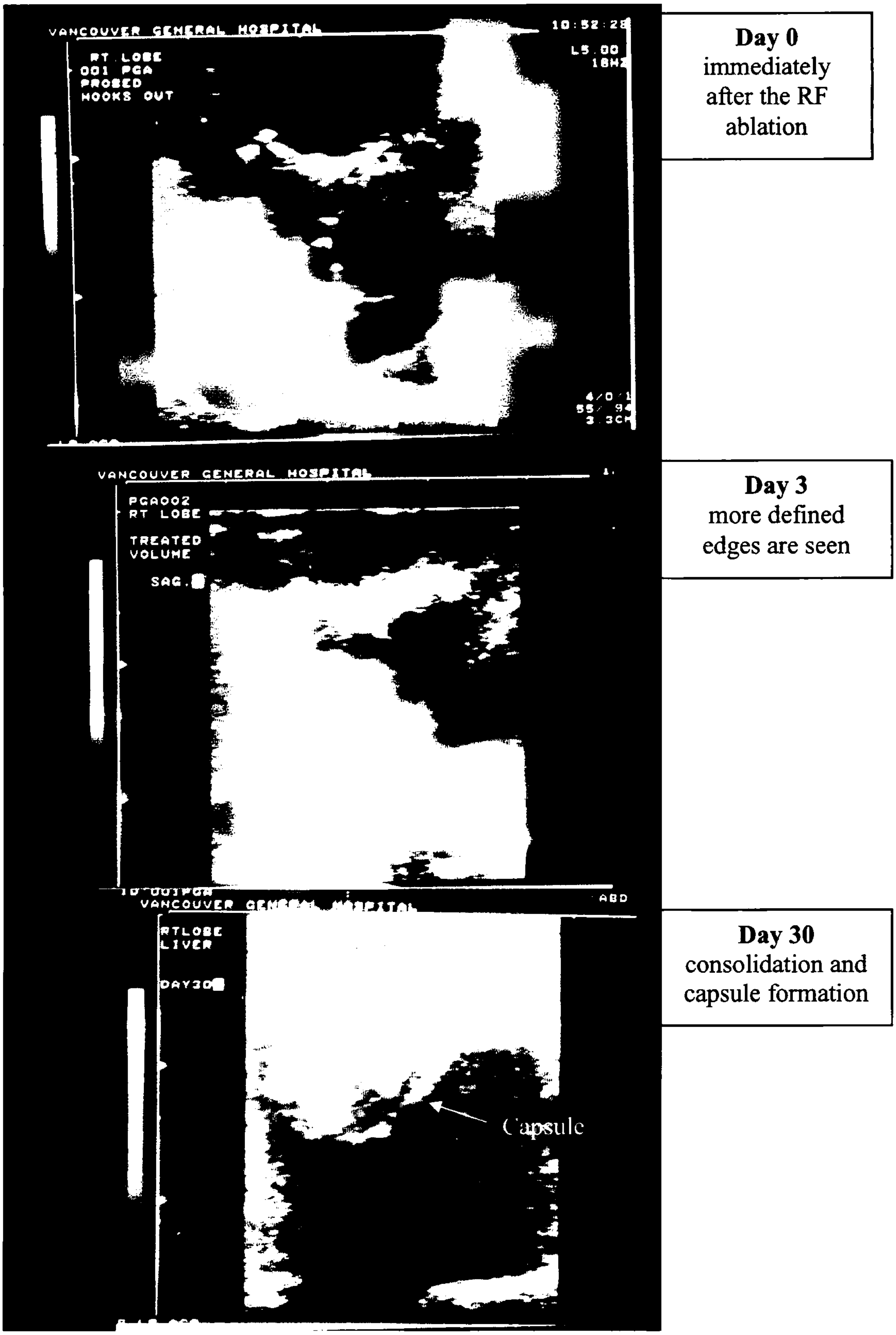

Figure 18. The RF ablation at 3 and 30 days post RFA follow up with the US exam in animal from PGA group.

CHAPTER FOUR

4. Discussion

4.1 Overview and general comments

The experiments were completed according to the described experimental methodology. Despite large technical components like double laparotomies, left segmental lobectomy and multiple exams with US at each phase of the study only three animals either died or had to be euthanised during the study. The remaining animals tolerated procedures well and all gained weight according to the growth pattern expectations between 14 – 22 kg/month. There have been no previous studies addressing short and long-term survival after the RF ablation in animals. This is the first attempt to assess the clinical application of the multi-prong RF electrode. All the data parameters of the radiofrequency ablation were also evaluated by the engineering group at the RITA Medical Instruments development department, with the purpose of improvement in the data collection and real-time data feedback and new software development.

4.2 Radiofrequency ablation

The RF electrode proved to be technically simple to deploy and control during the procedures. Despite a temperature of 50°C being high enough to cause local tissue necrosis, it was obvious that with a multi-prong electrode there is a component of tissue between the prongs that needs higher current delivery to achieve ablation. The ability of RF to create changes within high blood flow tissue like liver has been known since early studies on bovine cadavers and guinea pig models. However those experiments addressed only the single straight electrode. In our experiments the so-called "common treatment temperature" had to be much higher to produce effective RF ablation. The minimum temperature of 50°C was high enough to create localized areas of reddened appearance, sometimes of very small size. The area of so-called white appearance was present only in 30% of these low-temperature ablations. The temperature at 60°C was more effective in creation of 'pale' areas around the prongs, however it was not enough to create areas of ablation confluence. Only the RF ablations with a common treatment temperature of at least 70°C consistently created confluent peri-electrode coagulative necrosis ($p<0.001$). This is a significant finding as it applies to the clinical application of this technology. The triple or future multiple-prong models have to consider in its technology the volume of the tissue to be ablated. The minimum temperature should be 70°C, however in many cases this may still be too low to provide predictable ablation volume of the tissue most distant from the prongs. Liver tumours around or close to larger vessels or diaphragm treatment will require even higher temperatures to be successful. On the other hand the additional procedures causing temporary reduction of the blood flow, like Pringle's portal triad occlusion, may be utilized and its effects need to be investigated.

The results recorded with the real-time data software indicate differences between the experimental groups in the time needed to complete the successful ablation, and amount of the energy delivered to the tissue. The main reason appears to be a difference in anatomy of placement area of the electrode. The area close to the main hepatic vein usually has one large vessel and smaller branches, so beside single large flow vessel, the remaining vessels are too small to effectively compromise the tissue heating. The hepatic vein flow is a low pressure and relatively slow, passive flow system. This translated into a shorter time of effective treatment temperature during creation of the ablation and lower requirements for energy needed to achieve this goal. In the PGA group this was 6.5 minutes (this time was downloaded from the real-time software retaining data in 30 seconds intervals). On the other hand, areas of liver tissue close to the portal vein branches and terminal branches of the hepatic artery contain high pressure and high flow vessels. In addition, extension of the Glisson's capsule in form of the sheath of connective tissue around the vessels is an effective temperature insulator. For this reason all ablations in this particular area required longer application of the current to create desired lesions, which were either palpable by hand or somewhat poorly imaged by US. The total amount of energy was related to the extended time of the procedure. The ablation in the PGD group was successful in all the animals. The temporary changes in the diaphragm tissue were consistent with expectations. An increased time of ablation was needed due to either transcapsular attempt at injuring the diaphragm or one prong being positioned out of the parenchyma of the liver. The organ surface interfaces are known to be a limiting factor in the transfer of any current energy as the tissue impedance is different for each of the tissue type and especially with air around the exposed prong. The ability to reach the common temperature is compromised in those cases because of non-uniform feedback on remaining prongs and unexpected and difficult to control rise in the impedance of given tissue types. In addition, it was generally unpractical to alter the positions of all the prongs during the RF ablation. As long as the tips of electrode are embedded in the tumour or targeted tissue the imaging role is to identify the possible trouble spots like large vessels, gallbladder, diaphragm or collateral structures to avoid direct RF current flow through undesired areas. The interposition of parenchymal structures like vessels and bile ducts in the tumour or at its periphery is to be expected. The size of the vessels and volume of the blood flow will be a critical part in the effectiveness of the RF ablation. But as in all RF ablations in this study, the small vessels (<2 mm diameter) were ablated, when within the geometry of the ovoid ablation around the RF probe. In contrast, the larger vessels were almost totally protected from effective coagulation. It was obvious that with the triple prong model the areas between prongs were sensitive to vessel related modulation of the RF ablation induced shapes. The ablations were performed in normal liver tissue, which in the clinical scenario is not a primary target for this technology.

The physics of RF current flow through the tissue follow the previously described rules, so the effectiveness of the ablation is dependent on the time of the current delivery, its power and tissue resistance. We did not experience interrupted ablation due to extremely high impedance, the highest was recorded in the PGX group at 117.4 Ohms, but the ablations in this group were performed with different goal in mind. In the more physiological groups like PGA, PGB or PGD the mean impedance of the tissue was in the range of 73 – 97.8 Ohms. There was no evidence of excessive charring on the tips or around them after the completion of the RF ablation. The presence of so-called steam bubbles formation was evaluated with one separate experiment and this phenomenon was found to be of no clinical significance.

The role of the impedance in the successful RF ablation has been described before, but it did not present any complications in our model [64]. Overall the ablations were performed without any technical difficulties. The manual increase of the power during the initial 3 minutes until temperature of 70°C could be replaced in newer models of generators with impedance-temperature feedback and performed automatically. The liver tissue is a good environment for RF ablation technology. It provides significant volume of tissue as a collateral buffer and any liver mass can be accessed in any of the approaches either open, laparoscopic or percutaneuos.

4.3 Clinical outcomes

The group of 28 animals, with exclusion of the 3 who developed complications unrelated to RF ablation technology, did very well. All the animals gained weight according to their age and growth pattern. The significance of this finding is that despite extensive experimental surgery the potential side effects of RF or its long-term complications were of lesser degree than the recovery from laparotomy and segmental liver resection. The ablation effects, especially between days 3 and 30 although interesting scientifically were of no clinical significance. The clinical conclusion may be drawn that, if needed, open RF ablation may be utilized in patients during staging laparotomy or when the tumour characteristics are not favourable for liver resection and a percutaneous approach is contraindicated.

4.4 Ultrasound as the imaging tool

The efficacy of ultrasound as imaging tool has been accepted and interpretation of lesions is improving. The ability to guide the RF probe was very good, especially in direct application on the surface of the liver capsule. The group best to follow, because of the most obvious tissue changes, was the PGX group with its large energy ablations. All of the lesions in this group were measurable on day 3. Then with the progress of healing and retraction of the lesion the identification became more uncertain. The remaining groups had the best US delineation at day 3 as well. This finding is most likely related to the tissue changes at this stage with a sharp edge demarcation and tissue edema in the area of RF ablation. Overall 32.4% (N=11) of RF lesions were measurable on Day 0, after RF ablation, 47.5% (N=20) on day 3 and 28.6% (N=8) on day 30. Despite these differences between the groups there was no significant statistical difference. In general US is a good technology for guidance of the RF electrode application. The early follow-up in the most immediate postoperative period is well documented with US imaging, which in some groups was 75-100% accurate. Long-term follow up is less effective, but this is mostly due to the healing changes and retraction and scaring of the tissue.

As during most of the studies there was an intravascular phenomenon observed in the form of echogenic images appearing in the vessel during the RF ablation. The so-called 'bubbles' of gas, were entering the circulation and moving even against the flow of blood, when the temperature of the ablated tissue, were reaching as high as 90°C. Sometimes echogenic findings were accumulating in the branch of the vessel or its bifurcation. When the temperatures dropped the images disappeared (Fig. 19). To investigate this particular observation, an additional trial RF ablation was performed with a shunt of the blood through a micro filter to exclude clot formation. The RF current delivery was performed in prolonged manner and the bubbles were identified on US images. Despite the effective shunt we did not find any clots or tissue particles in the circulation. This imaging phenomenon has to be explained as temporary vapor formation, when the tissue temperatures reach sub-boiling levels. Its behaviour, gravity like regulated (moving against the blood flow, accumulating around bifurcations etc), is consistent with physical qualities of fluid vapor, which may behave like a warm fluid bubble in a cooler surrounding. The clinical significance of this observation is limited, however the exact importance is currently unknown.

4.5 Histopathology

The tissue changes induced by RF ablation are consistent in what was anticipated. Coagulative necrosis is well defined. The edges of the ablation are sharp with minimal transition between the ablation and viable tissue, in most cases measuring only one or two cells. All samples reviewed had the same pattern of tissue changes on day 0, 3, and 30 regardless of the study group. The zonation was uniform with its maximal presentation on day 0 and no zonation on day 30. The sizes of 'reddened' and 'pale' zones were dependent on the position of the probe and somewhat uneven. However this was within the predictable pathology exam pattern. The tissue changes in the acute phase day 0 to day 3 were characteristic of coagulative necrosis in all the cases. The nuclear and cytoplasmic changes were consistent and indicated total necrosis of the ablated tissue. The zones of the reddened or palor are both zones of total tissue necrosis. Their gross and microscopic difference is due to the loss of staining of the hemoglobin containing erhytrocytes. The more central zone of palor is the area of much longer exposure to the RF current flow than more peripheral reddened zone. The reddened zone

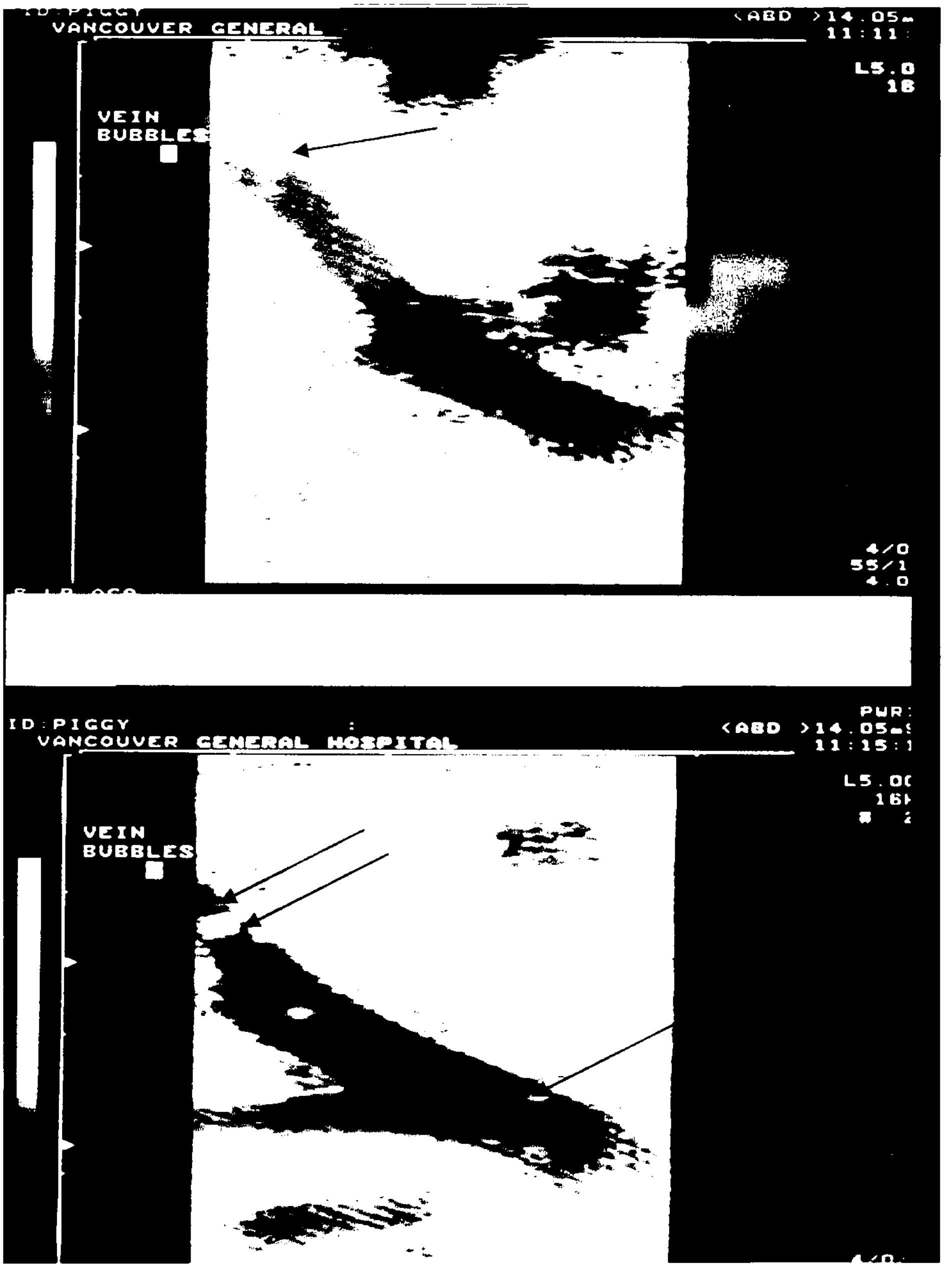

Figure 19. Ultrasound images of so called 'gas bubbles" representing the hyperechoic images of the intravascular flow of the interstitial fluid vapor dissipating away from the area of RF ablation (arrows).

proteins, especially in the erythrocytes, are denaturated, but still not damaged enough so that they will stain with H+E. Both zones are necrotic and this has been consistently confirmed with the NADH staining. In all cases NADH histochemistry indicated no staining within these zones out towards the periphery of the reddened zone. Eventually the conclusion was reached that what we see with the naked eye accurately predicts the extent of RF ablation.

Day 30 samples were evaluated in all animals. All indicated a reasonable recovery after the RF ablation. There were no signs of any complications present. No hematoms, hemorrhages, bile leaks, bilomas, or infections were identified in this study. The residual necrotic tissue was identified in all the cases. Capsule formation was present in all the cases, but its thickness was inconsistent. Some lesions had a capsule up to 1 mm thick. Such resolution to almost full, uncomplicated recovery carries a significant clinical importance. The ability of the liver tissue to recover after RF ablation with minimal functional consequence allows for using the RF in liver tumours with little concern about long-term surrounding tissue health and function.

The resilience of the vascular wall to permanent damage by RF ablation is worth mentioning. The transient small thrombi and local wall inflammatory cell infiltration proves a potential for good recovery of the vessels even if within the ablation area. On the other hand the 'sink effect' plays also a protective role. The small size vessels carry a low risk of becoming a source of major thrombus, and vessels < 2mm in size are usually totally coagulated when present within the RF ablation.

The unintentional placement of the prongs into the diaphragm has been always a reason for concern. The diaphragm is quite intensively innervated especially in the areas covered by peritoneum. The localized thermal injury may be the cause of perforation, malfunction, and long-term respiratory complication such as plural effusion or empyema. The results from group PGD proved that despite being it most likely a painful experience the diaphragm injury heals almost without consequences and complications.
Delivery of an excessive amount of the RF energy to the tissue was investigated with the most powerful generator currently available. All animals did well, and clinically were without any complications. One case of complex, non-infected cyst was identified. There was no bleeding and no bile leak was noticed. Interestingly in one of the PGB cases (PGR) the resolution of the necrosis was a small mass with collateral deformation of the surrounding structures. In this case an infarct of Zahn was diagnosed. The infarct of Zahn is a wedge shape discoloration to the surface of the transsected liver parenchyma. This is a consequence of interruption of one of the blood supply systems to the liver, either arterial vessel or portal vein branch occlusion. In this particular case scar deformed the anatomy of the branches of portal vein leading to localized ballooning of the veins. It is known that presence of the infarct of Zahn is of no clinical significance as majority of them are diagnosed incidentally in humans at autopsy.

New future RF ablation probes should be equipped with self-regulated software managed circuit of safety based on the impedance, temperature and time feedbacks. Overall the RF ablations in all the groups were safe and resulted in consistent pattern of the tissue changes both in the acute phase and the long-term phase. The liver regeneration and healing potential is one of the mechanisms that will allow good recovery for this organ treated with RF ablations. As all the animals underwent two RF ablations each, the conclusion can be made that human trials are also feasible in cases of multiple tumours in the liver.

CHAPTER FIVE

5. Summary and conclusions

This is the first scientific study to recreate environment to assess possible RF injuries to intrahepatic and extrahepatic structures in porcine model. We were able to evaluate RF ablations in different areas of animal liver and successfully survive animals. The overall safety of multiple RF ablations was confirmed by not experiencing RF related deaths or complications in the animals.

5.1 RF and related complications

There was no evidence of bile leak, bilomas or hemorrhage after RFA as the frequency of these complications was zero. The recovery of the normal liver tissue after RFA is almost complete and resolution of the necrotic tissue does not indicate any potential for delayed tissue infection or cyst formation. This has a critical importance when considering RF ablations of liver tumours, especially when adjacent area of liver is ablated during treatment [79].

The type of injury to the vessel wall observed in the study confirms that it is of transient nature. Small thrombi in small caliber vessels may be of no clinical significance in the RFA of human liver. Thrombosis of large blood volume flow vessels was not recorded and could be considered unlikely in clinical application of RF. One case of so-called infarct of Zahn should serve, however, as a remainder that in isolated cases the permanent rearrangement of liver circulation may be created as a result of RFA.

The results in the diaphragmatic injury group proved that the thermal injury to the diaphragm is created in all cases when the prongs are close to this vital structure. The extent of injury may vary, but it is temporary. Obviously painful after RFA, diaphragmatic muscle will recover without functional or clinical sequel in most of the cases.

5.2 Radiofrequency current

RF current requirements were different according to the placement of the probe, however due to small number of cases, the specifics of this relationship should be evaluated in further studies. It is clear that the amount of delivered energy may not be the best feedback tool to assess the volume of created tissue ablation. One may conclude that a combination of power, electrode-tip temperature and most likely the speed of change in tissue impedance are the factors to focus on during the up coming studies to better understand and improve the effectiveness and safety of new generation RF electrodes.

5.3 Radiofrequency and liver tissue necrosis

We proved that the tissue ablation in the liver creates similar picture of coagulative necrosis in all the areas of the liver. Their resolution and recovery follow similar pathway and stages as described by observations on day 3 and day 30. The long-term outcome is good and functional deterioration of the organ was unseen.

5.4 Role of ultrasound in RFA

Ultrasound is a very good method of guidance and localization on the RF probe. It is also effective in identifying the RF lesion in early post RFA period. The effectiveness in measurement of lesions' size and follow up imaging is less than satisfying.

5.5 Summary

In summary, the results of this study proved that radiofrequency ablation is safe in the porcine model. It is also very effective in creating volume necrosis in normally perfused liver. Its safety in clinical application in human liver should be still investigated. The likelihood of injuring the collateral organs around liver is low, but present. Beside percutaneous approach [80,81], laparoscopic [82] and open application of RFA should be considered especially in cases of subcapsular liver tumours.

5.6 Future consideration

The effect of blood flow in the form of Pringle vascular occlusion on effectiveness of RF will be investigated during next series of the experiments. The clinical application in cases of human liver tumours will be performed on the experimental basis in selected cases in the near future.

Positive results of this study should stimulate assessment of RFA efficacy in tissue of other organs such as lungs, kidneys and spleen in selected animal models.

5.7 Presentations and publications of the thesis material and results

The observations and results of this study were presented in parts and in total during peer-reviewed meetings as follow:

1. Effect of temperature on RF tissue ablation.
   EJ Patterson, ***AK Buczkowski***, D Owen, A Nagy, CH Scudamore
   III World Congress of Heptopancreatic Surgery, Madrid, Spain, May 26, 1998
   Endoscopic and Minimally Invasive Surgery Congress, Rome, Italy, June 4, 1998

2. Safety Study of Hepatic RFA in an Animal Model.
   AK Buczkowski, CH Scudamore, EJ Patterson, D Owen
   XIII Annual Scientific Session of the Academy of Surgical Research
   San Antonio, Texas, September 4-6, 1997

3. Pathology of RFA in an Animal Model.
   AK Buczkowski, CH Scudamore, EJ Patterson, D Owen
   XIII Annual Scientific Session of the Academy of Surgical Research
   San Antonio, Texas, September 4-6, 1997

4. Radiofrequency of Porcine Liver in Vivo.
   AK Buczkowski, CH Scudamore, AG Nagy, DA Owen, EJ Patterson
   XIII Annual Scientific Session of the Academy of Surgical Research
   San Antonio, Texas, September 4-6, 1997

5. Usefulness of Ultrasound in Animal Model of Hepatic Radiofrequency Ablation.
   CH Scudamore, ***AK Buczkowski***, EJ Patterson, D Scallion, J Backley, D Owen
   VIII Congress of World Federation of Ultrasound in Medicine and Biology.
   Buenos Aires, Argentina, September 1-5, 1997

6. Prevention of Injuries to Intrahepatic and Perihepatic Structures with Radiofrequency Probe. ***AK Buczkowski***, EJ Patterson, DA Owen, D Breen, CH Scudamore. Society of American Gastrointestinal-Endoscopic Surgeons, San Diego, California, March 21-22, 1997

Publications:

1. Safety of Hepatic Radiofrequency Ablation in an Animal Model. ***AK Buczkowski***, EJ Patterson, AG Nagy, D Scallion, DA Owen, CH Scudamore Surgical Endoscopy (under review, 2002).

Note:

The results of this study were submitted to Federal Drug Administration (FDA) in 1997 as part of the documentation addressing RFA safety in animals. It was used for federal approval of RF technology for liver cancer treatment in humans. The approval was granted in 1998.

BIBLIOGRAPHY

1. Parkin DM, Muir CS, Whelan SL et al. Cancer incidence in five continents. IARC Publication No. 120, Lyon, International Agency for Research on Cancer, 1997.
2. Bosch FX, Ribes J, Borras J. Epidemiology of primary liver cancer. Semin Liver Dis 1999;13:271-280.
3. Scarantino C, Hoffman L, Omitz R, Enterline D, Metastases and disseminated disease. In: Rubin P., ed. Clinical oncology: a multidisciplinary approach for physicians and students. Philadelphia: W>B> Saunders, 1993:677-89.
4. Ravikumar T, Kane R, Cady B, Jenkins R, Clouse M, Steele G. A 5-year study of cryosurgery in the treatment of liver tumours. Arch Surg 1991;126:1520-4.
5. Sheiner PA, Brower ST. Treatment of metastatic cancer. Semin Liver Dis, 1994;14:169-175.
6. Hughes K, Scheele J. Surgery for colorectal cancer metastatic to the liver. Surg Clin North Am 1989,69:339-345.
7. Barr LC, Skene AI, Thomas JN. Metastectomy. Br J Surg,1992;79:1268-73.
8. Livraghi T, Bolondi L, Lazzarnnis P, et al. Percutaneous ethanol injection in the treatment of heaptocellular carcinoma in cirrhosis: A study on 237 patients. Cancer 1992;69:925-29.
9. Shiina S, Tagawa K, Niwa Y et al. Percutaneous ethanol injection therapy for heaptocellular carcinoma: Results in 146 patients. Am J Roentgenol 1993;160:1023-28.
10. Bischof J, Christov K, Rubinsky B. A morphological study of cooling rate response in normal and neoplastic human liver tissue: Cryosurgical implications. Cryobiology 1993;30:482-92.
11. Funovica JM, Fritsch A, Herbst F et al. Primary hepatic cancer: The role of limited resection and total hepatectomy with orthotopic liver replacement. Hepatogastroenterology 1988;35:316-21.
12. Gage AA. Cryosurgery in the treatment of cancer. Surg Gynecol Obstet 1992;174:73-92.

13. Cedrone A, Rapaccini G, Pompili M, Grattagliano A, Aliotta A, Trombino C Neoplastic seeding complicating percutaneous ethanol injection for treatment of hepatocellular carcinoma. Radiology 1992;183:787-8.
14. D'Agostino H, Solinas A. Percutaneous ablation therapy for hepatocellular carcinomas. AJR Am J Radiol 1995;164:1165-7.
15. Ebara M, Ohto M, Sugiura N, Kita K, Yoshkawa M, Okuda K, Kondo F, Kondo Y. Percutaneous ethanol injection for the treatment of small hepatocellular carcinoma: study of 95 patients. J Gastroenterol Hepatol 1990;5:616-26.
16. Goletti O, De Negri F, Pucciarelli M, Sidoti F, Bertolucci A, Chiarugi M, Seccia M. Subcutaneous seeding after percutaneous ethanol injection of liver metastases. Radiology 1992;183:785-6.
17. McKinnon JG, Temple WJ, Wiseman DA, Saliken JC. Cryosurgery for malignant tumors of the liver. Canadian Journal of Surgery 1996;39:(5):401-6.
18. Ravikumar T, Kane R, Cady B, Jenkins R, Clouse M, Steele G. A 5-year study of cryosurgery in the treatment of liver tumours. Arch Surg 1991;126:1520-4.
19. Rossi S, Di Stasi M, Buscarini E, Cavanna L, Quaretti P, Squassante E, Garbagnati F, Buscarini L. Percutaneous radiofrequency interstitial thermal ablation in the treatment of small hepatocellular carcinoma. Cancer Journal of Scientific American 1995;1:73-81.
20. Shiina S, Tagawa K, Unuma T, Komatsu Y, Yoshiura K, Hamada E, Takahashi M, Shiratori Y, Terano A, Omata M, Kawauchi N, Inoue H. Percutaneous ethanol injection therapy for hepatocellular carcinoma. AJR 1993;160:1023-8.
21. Amin Z, Donald JJ, Masters A et al. Hepatic metastases: interstitial laser photocoagulation with real-time US monitoring and dynamic CT evaluation of treatment. Radiology 1993;187:339-47.
22. Nolsoe CP, Torp-Pederson S, Burcharth F, et al. Interstitial hyperthermia of colorectal liver matastases with US-guided Nd-YAG laser with a diffuser tip: A pilot clinical study. Radiology 1993;187:333-37.
23. Liver Cancer Study Group of Japan. Primary liver cancers in Japan. Cancer 1980; 45:2662-2669.

24. Lai EC, Fan ST, Lo CM, et al. Hepatic resection for hepatocellular carcinoma. Audit of 343 patients. Ann Surg 1995; 221:291-298.
25. Al-Hadeedi S, Choi TK, Wong J. Extended hepatectomy for hepatocellular carcinoma. Br J Surg 1990; 77:1247-1250.
26. Kanematsu T et al. A comparative study of hepatic resection and transcatheter arterial embolization for the treatment of primary hepatocellular carcinoma. Cancer 1993; 71:2181-2186.
27. Nagorney DM et al. Primary hepatic malignancy: surgical management and determinants of survival. Surgery 1989; 106:740-749.
28. Patt YZ, et al. Hepatocellular carcinoma: a retrospective analysis of treatments to manage disease confined to liver. Cancer 1988; 61:1884-1888.
29. Cady B, Stone MD, McDermott WV JR, et al. Technical and biological factors in disease-free survival after hepatic resection for colorectal metastases. Arch Surg 1992; 127:561-569.
30. Hughes KS, et al. Resection of the liver for colorectal carcinoma metastases: a multi-institutional study of indications for resection. Surgery 1988; 103:278-288.
31. Scheele J, Stangl R, Altendorf-Hafman A. Hepatic metastases from colorectal carcinoma: impact of surgical resection on the natural history. Br J Surg 1990; 77:1241-1246.
32. Petrowsky H, Gonen M, Jarnagin W et al. Second liver resections are safe and effective treatment for recurrent hepatic metastases from colorectal cancer; A bi-institutional analysis. Ann Surg 2002, 235(6):863-871.
33. Choti MA, Stzman JV, Tiburi MF et al. Trends in long-term survival following liver resection in hepatic colorectal metstases. Ann Surg 2002,235(6):759-766.
34. Onishi K, Ohyama N, Ito S, et al. Small hepatocellular carcinoma: treatment with US-guided intratumoral injection of acetic acid. Radiology 1994; 193:747-752.
35. Tian JH, Xu BX, Zhang JM, et al. Ultrasound-guided internal radiotherapy using yttrium-90 glass microshperes for liver malignancies. J Nucl Med 1996; 37:958-963.
36. Huang JF, Kuang M, Lu MD, et al. Percutaneous hyperthermal distalled water injection therapy (PHDT) for liver cancer. Asian J Surg 1999; 22:337-341.

37. Mok TSK, Kanekal S, Lin XR, et al. Pharmacokinetic study of intralesional cisplatin for the treatment of hepatocellular carcinoma. Cancer 2001; 91:2369-2377.

38. Seki T, Wakabayashi M, Nakagawa T, et al. Ultrasonically guided coagulation therapy for patients with small hepatocellular carcinoma:comparison with percutaneous ethanol injection therapy. Cancer 1999; 85:1694-1702.

39. Rossi S, Fornari F, Buscarini L. Percutaneous ultrasound-guided radiofrequency electrocautery for the treatment of small hepatocellular carcinoma. J Interv Radiol 1993; 8:97-103.

40. Livraghi T, Goldberg SN, Lazzaroni S, et al. Small hepatocellular xarcinoma: treatment with radiofrequency ablation versus ethanol injection. Radiology 1999; 210:655-661.

41. Ikeda M, Okada S, Ueno H, et al. Radiofrequency ablation and percutaneous ethanol injection in patients with small hepatocellular carcinoma: comperative study. Jpn J Clin Oncol 2001; 31:322-326.

42. Curley SA, Izzo F, Ellis LM, et al. Radio-frequency ablation of hepatocellular cancer in 110 patients with cirrhosis. Ann Surgery 2000; 232:381-391.

43. Lencioni RA, Cioni D, Donati F et al. Percutaneous treatment of small hepatocellular carcinoma in cirrhosis: radiofrequency thermal ablation vs. ethanol injection – a prospective, randomized trial. Radiology; 213(suppl):123.

44. Shiina S, Teratani T, Obi S et al. Prospective randomized controlled trial comparing percutaneous radiofrequency ablation and percutaneous ethanol injection therapy for small hepatocellular carcinoma. Gastroenterology 2000; 118(Suppl):959.

45. Olschewski M, Lencioni R, Allgaier H et al. A randomized comparison of radiofrequency thermal ablation and percutaneous ethanol injection for the treatment of small hepatocellular carcinoma. Pro AM Soc Clin Oncol 2000;abstract 500.

46. Llovet JM, Vilana R, Bru C, et al. Increased risk of tumour seeding after percutaneous radiofrequency ablation for single hepatocellular carcinoma. Hepatology 2001; 33:1124-1129.

47. Kato T, Reddy KR. Radiofrequency ablation of hepatocellular carcinoma: help or hazard? Hepatology 2001; 33:1336-1337.

48. Bolondi L, Gaiani S, Celli N et al. Tumour dissemination after radiofrequency abaltion of hepatocellular carcinoma. Hepatology 2001; 34:608.

49. Solbati L, Goldberg SN, Ierace T et al. Hepatic metastases: percuraneous readio-frequency ablation with cooled-tip electrodes. Radiology 1997; 205:367-373.

50. Rossi S, Buscarini E, Garbagnati F et al. Percutaneous treatment of small hepatic tumours by expandable RF needle electrode. Am J Roentgenol 1998; 170:1015-1022.

51. Brown KT, Brody LA. Percutaneous methods for ablation of hepatic neoplasm. In Blumgart LH, Fong Y eds. Surgery of the liver and biliary tract. London: W Saunders Co., 2000:1565-1576.

52. Adam R, et al. Place of cryosurgery in the treatment of malignant liver tumours. Ann Surg 1997; 225:38-9.

53. Bilchil AJ, et al. Cryosurgery causes profound reduction in tumour markers in hepatoma and noncolrectal hepatic metastases. Ann Surg 1997; 63:796-800.

54. Zhou XD, et al. An 18-year study of cryosurgery in the treatment of primary liver cancer. Asian J Surg 1992; 15:43-47.

55. Ryu M, et al. Therapeutic results of resection, transcatheter arterial embolization and percutaneous transhepatic ethanol injection in3225 patients with hepatocellular carcinoma: a retrospective multicenter study. Jpn J Clin Oncol 1997; 27:251-257.

56. Yamada R, et al. Transcatheter arterial embolization in unresectable hepatocellular carcinoma. J Cardi9ovasc Intrervent Radiol 1990; 13:135-139.

57. Ebra M, et al. Percutaneus ethanol injection for the treatment of hepatocellular carcinoma: study of 95 patients. Gastroenterolo Hepatol 1990; 15:615-626.

58. Lencioni R et al. Long-term results of percutaneous ethanol injection therapy for hepatocelluar carcinoma in cirrhosis: A European experience. Eur Radiol 1997; 7:514-519.

59. Couinaud C. Lobes et segments hepatiques: notes sur architecture anatomique et chirurgicale do foie. Presse Med 1954,62:709.

60. McClusky DA, Skandalakis LJ, Colborn GL, Skandalakis JE. Hepatic surgery and hepatic surgical anatomy: historical patterns in progress. World J Surg 1997,21:330-342.

61. Response to cellular injury. By JR Goepel in JCE Underwood, General and Systemic Pathology, Churchill Livingstone 1992 (First edition).
62. Wound healing. By Fine NF, Mustoe TA in LJ Greenfield, Surgery, Lippincott-Raven 1997 (Second edition).
63. Strohbehn JW, Temperature distribution from interstitial RF electrode hyperthermia systems: theoretical predictions. Radiation Oncology Biol. Phys., Vol 9,1983, 1655-1667
64. Organ LW. Electrphysiologic principles of radiofrequency lesion making. Int Symp Radiofrequency Lesion Making Procedures, Chicag, Ill, 1976, Appl Neurophysiol 39: 69-76
65. d'Arsonval A. Action physiologique des courants alternatifs. Comp Rend Soc Biol 1891; 43:283.
66. d'Arsonval A. Action physiologique des courants alternatifs agrande frequence. Arch Physiol Norm Path (5th) series 1893; 5:401-408.
67. d'Arsonval A. Production des courants de grande intensite; leurs effects physiologiques. CR Seances Soc Biol Ses Fil 1893; 45:122-124.
68. Riviere AJ. Actions des courants de haute frequence et des effluves du resonateur oudin sur certaines tumours malignes et sur tiberculose. J Med Int 1990; 4:776-777.
69. Beer E. Removal of neoplasms of the urinary bladder: a new method employing high frequency (Oudin) currents through a cauterizing cystoscope. JAMA 1910; 54:1768-1769.
70. Beer E. Discussion of advancecs insurgery, HA Kelly and GE Ward. Arch Phys Ther, X-Ray, Radium 1931;12:471-472.
71. Christie RV, Benger CA. Experimental study of diathermy. J Exp Med 1927; 46:715.
72. Huntoon RD. Tissue heating accompanying electrosurgery: an experimental investigatio. Ann Surg 1937; 195:270-290.
73. Hahn DE. The biophysics of radiofrequency catheter ablation in the heart: the eimportance of temperature monitoring. PACE, Vol. 16:586-591.
74. AE Siperstein, A Gitomirski, History and Technology Aspects of Radiofrequency Thermoablation, Cancer J 2000; 6(Suppl 4):5293-5303.

75. Scudamore C. Volumetric radiofrequency ablation technical considerations. Cancer J Sppl 2000,6(s4):s316-s318. Scudamore C. Volumetric radiofrequency ablation technical considerations.

76. Lounsbarry W, GoldschmintV, Linke CA et al. The early histologic changes following electrocoagulation. J Urol 1961; 86:321-329.

77. Rossi S, Formari F, Paties C et al. Thermal lesions induced by 480 kHz localized current field in guinea pig and in pig livers. Tumori 1990; 1990;76:54-57.

78. McGahan JP, Brock JM, Tesluk H et al. Hepatic ablation with use of radio-frequency electrocautery in the animal model. J Vasc Interv Radiol 1992;3:291-297.

79. McGahan JP, Browning PD, Brock JM et al. Hepatic ablation using radiofrequency electrocautery. Invest Radiol 1990; 25:267-270.

80. Rossi S, Di Stasi M, Buscarini E, Quaretti P, Garbagnati F, Squassante L, Paties CT, Silverman DE, Buscarini L. Percutaneous RF interstitial thermal ablation in the treatment of hepatic cancer. 1996,AJR;167:759-68.

81. McGahan J, Scheider P, Brock J. Treatment of liver tumours by percutaneous rediofrequency elecrocautery. Seminars in Interventional Radiol,1993;10(2):143-9.

82. Buscarini L, Rossi S, Formari F, Di Stasi M, Buscarini E. Laparoscopic ablation of the liver adenoma by radiofrequency electrocauthery. Gastrointestinal Endoscopy, 1995;41(1):68-70.